Dust issues in nuclear fusion reactors

S. Ratynskaia

Space and Plasma Physics - KTH Royal Institute of Technology, Stockholm

Outline

- Motivation
- Dust-plasma interaction and surface processes → dust dynamics & life-time
- Keys aspects of contact mechanics models for dust-wall collisions and adhesion / remobilization
- Summary

Motivation

- ITER dust → Be **(?)** and W
- DEMO dust → W

Amount of solid dust in fusion reactors is limited by safety regulations: dust can be

- tritiated
- toxic (Be)
- chemically active (e.g. with water vapour, production of H_2 and risk of explosion)

Nuclear licensing imposes in-vessel inventory limits:

- in ITER mobilizable dust limit is 1000 kg
- but much smaller amounts allowed on hot surfaces

Thus metallic **droplet/dust survival and dust inventory** is of main concern

Dust inventory evolution in fusion reactors

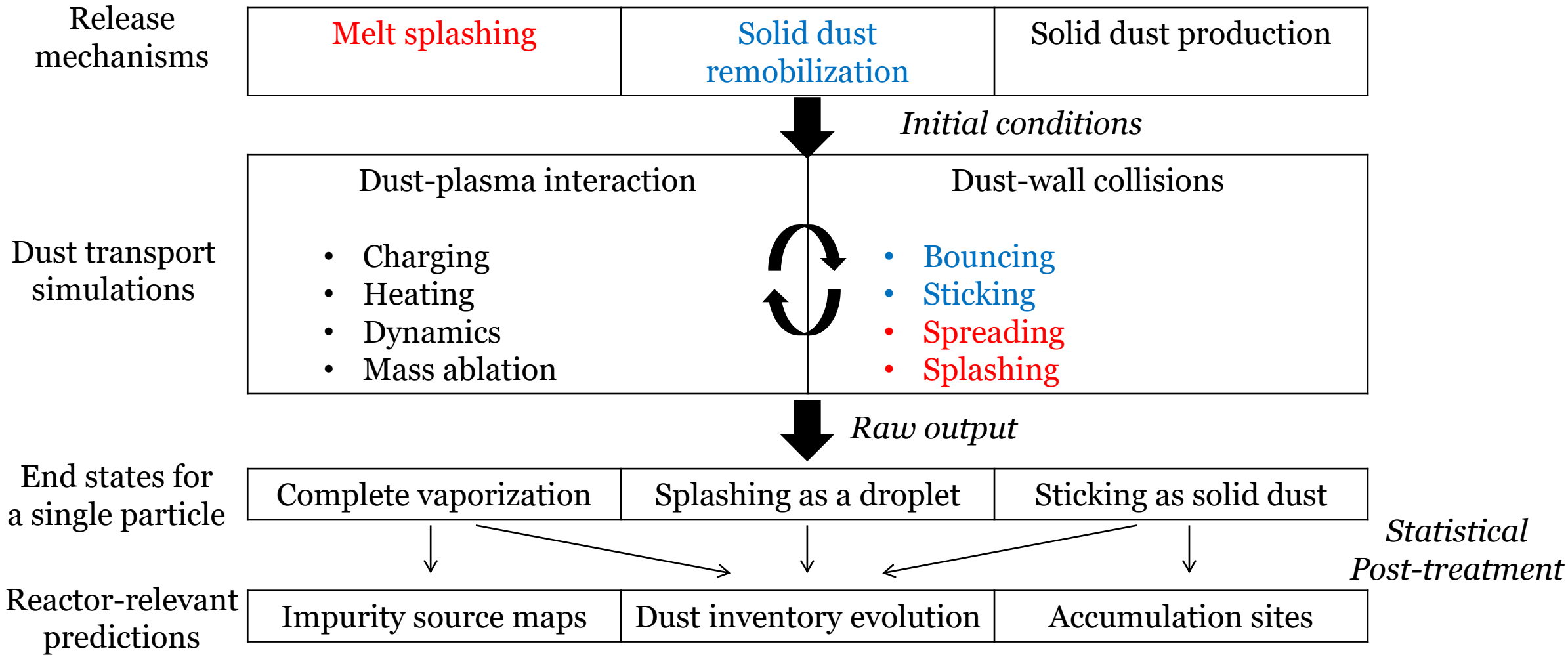

Fluid dynamics problems
Contact mechanics problems

Melt events in fusion devices – source of droplets

K. Krieger et al
Nuclear Fusion **58** (2018)

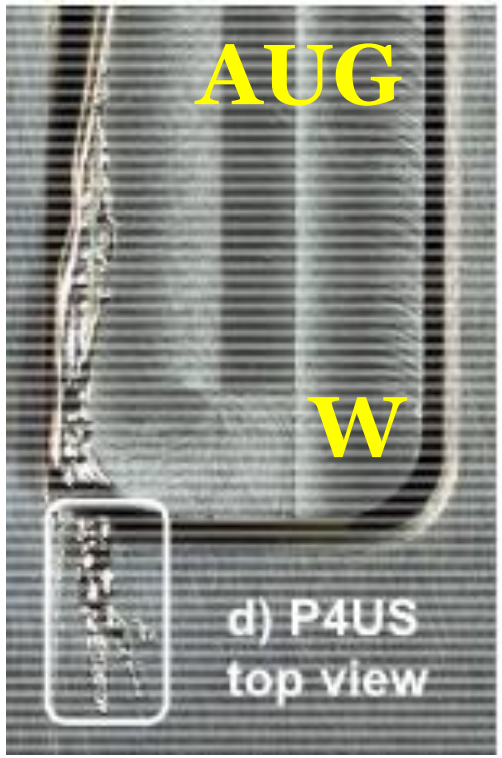

Unstable liquid pools → droplet ejection

Be molten layer
$h = 200\ \mu m, v = 3\ m/s$

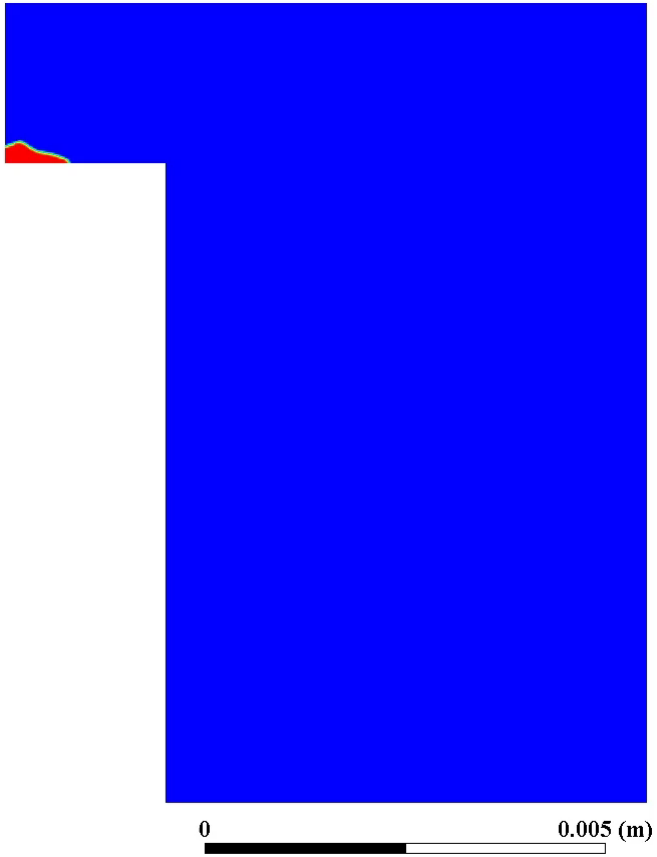

_metal) (Time=2.0033e-04)

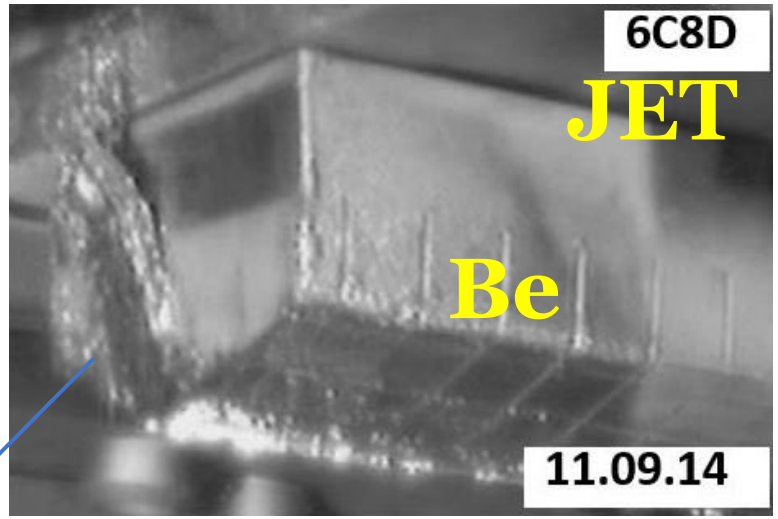

Jepu *et al* *Nuclear Fusion* **59** (2019)

Vignitchouk, Ratynskaia, Pitts et al
Nucl. Fusion **62** (2022)

Dust transport studies

A spherical dust particle/droplet is injected with given initial conditions into a given plasma background

Generic equations for the time evolution of the dust position, mass, enthalpy/temperature and (floating) electric potential

$$M_\mathrm{d}\frac{\mathrm{d}^2\vec{r}_\mathrm{d}}{\mathrm{d}t^2}=\vec{F}_\mathrm{tot} \qquad \frac{\mathrm{d}M_\mathrm{d}}{\mathrm{d}t}=\Gamma_\mathrm{tot} \qquad \frac{\mathrm{d}H_\mathrm{d}}{\mathrm{d}t}=Q_\mathrm{tot} \qquad I_\mathrm{tot}(\varphi_\mathrm{d})=0$$

The total current and heating power include contributions from the relevant surface processes:
electron and ion collection, thermionic and electron-induced electron emission, ion-induced electron emission, ion neutralization and backscattering, thermal radiation, vaporization

$$I_\mathrm{tot}=I_\mathrm{e}+\sum_j I_{\mathrm{i},j}+I_\mathrm{EIEE}+I_\mathrm{IIEE}+I_\mathrm{TE}$$

$$Q_\mathrm{tot}=Q_\mathrm{e}+\sum_j\left(Q_{\mathrm{i},j}+Q_{\mathrm{i},j}^\mathrm{bs}+Q_{\mathrm{i},j}^\mathrm{neut}\right)+Q_\mathrm{EIEE}+Q_\mathrm{IIEE}+Q_\mathrm{TE}+Q_\mathrm{rad}+Q_\mathrm{vap}$$

The functional form taken by each of these contributions can vary depending on the length scale ordering between the dust size and the plasma species' Debye lengths, Larmor radii and collisional mean free paths.

Modelling of incident heat and surface cooling fluxes is carried out through the incident *particle* fluxes

Surface process - overview

- The physical processes by which condensed matter ejects electrons into the ambient:
  - ✓Electron induced electron emission (secondary electron emission, electron backscattering, quasi-elastic electron reflection)
  - ✓Ion induced electron emission (kinetic electron emission, potential electron emission)
  - ✓Thermal field emission (field electron emission, thermionic emission, thermally-assisted field emission, field-assisted thermionic emission)
  - ✓Photoelectric emission

- The physical processes by which condensed matter ejects atoms and ions into the ambient
  - ✓Surface evaporation
  - ✓Physical sputtering
  - ✓Ion backscattering
  - ✓Chemical sputtering

Thermionic emission

- Thermionic electrons are bound electrons that are ejected to the ambient from the interior of a metallic body mainly as a consequence of their thermal agitation.
- In thermionic emission (TE), electrons are mainly emitted by an entirely classical over-the-barrier mechanism when their normal kinetic energy exceeds the height of the surface potential barrier. The free electron theory of metals (assuming a non-interacting Fermi gas) is typically employed for the derivation of key results.

Herring C and Nichols M H 1949 Rev. Mod. Phys. **21** 185

- In general, there are different thermionic emission regimes that are dictated by the competition between quantum tunneling and over-the-barrier escape. The regimes can be formally defined in a plot of the surface temperature versus the accelerating field strength. If distinguishing between regimes is based on the field strength (*i.e.* at constant surface temperature)
  - Classical thermionic regime (no external accelerating *(for emitted electrons)* electrostatic fields)
  - Schottky regime (very weak external accelerating electrostatic fields)
  - Extended Schottky regime (weak external accelerating electrostatic fields)
  - Field-assisted thermionic regime (moderate external accelerating electrostatic fields)

[For plasma-facing components the last three of importance for future machines

Tolias, Komm, Ratynskaia, Podolnik, *NME* **25**, 100818 (2020)]

- The process is not quantified by a yield, since it is not caused by the incidence of particle fluxes. It is quantified by expressions for the emitted electron current density which strongly depend on the surface temperature, the material composition and the external normal electrostatic field.

Richardson-Dushman formula

$$J_{\mathrm{th}}(T_s) = A_{\mathrm{eff}}\, T_s^2 \exp\left(-\frac{W_{\mathrm{f}}}{k_{\mathrm{B}} T_s}\right).$$

TE electrons are (half) Maxwellian with $T = T_s$ → COLD

- The thermionic current density is very sensitive to the

i. material work function, since it quantifies the height of the surface barrier that is crossed by the valence electrons
ii. surface temperature of the body, since it quantifies the strength of the thermal excitations that lead to the over-the-barrier emission.

- Good thermionic emitters should have a low work function and a high boiling / melting point.

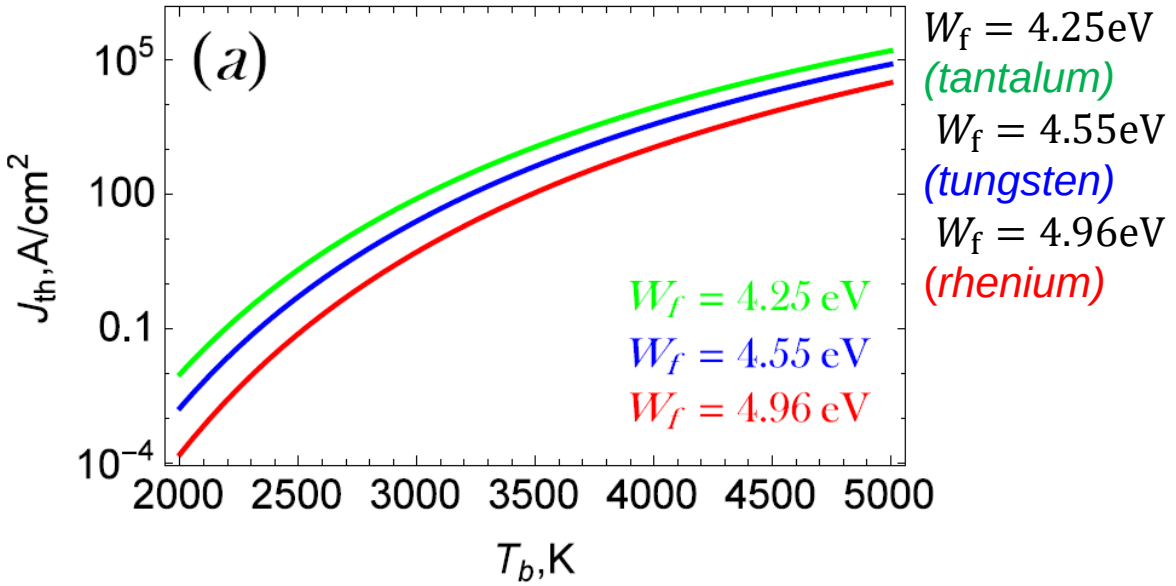

$W_{\mathrm{f}} = 4.25\mathrm{eV}$ *(tantalum)*
$W_{\mathrm{f}} = 4.55\mathrm{eV}$ *(tungsten)*
$W_{\mathrm{f}} = 4.96\mathrm{eV}$ *(rhenium)*

Surface cooling due to escaping thermionic electrons Γ_{th}

$$q_{te} = \Gamma_{th}(W_f + 2\, k_B T_s)$$

(filling the thermal vacancy)

NB: in plasmas escaping does not always follow Richardson-Dushman formula due to current limitation

Strongly emitting dust

- Well known for the planar wall case: “space-charge limited sheath”, “virtual cathode”, “potential well” [Hobbs and Wesson, *Plasma Phys.* **9** 85 (1967); Takamura et al, *Contrib. Plasma Phys.* **44** 126 (2004)]

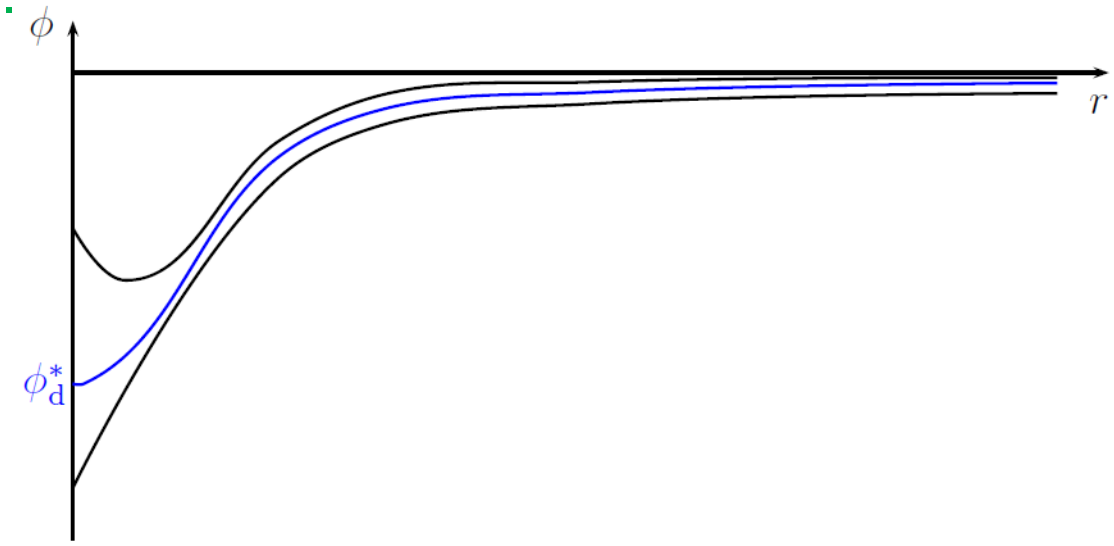

Emitted electrons bring their own length scales into the problem. Strong emission of **cold electrons → small Debye length**

Strongly emitting grain [Delzanno & Tang, *PRL* **113** 035002 (2014)]

OML+ model:

- Corrections only when the dust is positively charged
- Knowing the critical dust potential ϕ_d^* is enough
- Modify the OML trapped-passing boundary condition for emitted electrons only

Relation $Q_d = 4\,\pi\,\varepsilon_0\,r_d\,\phi_d$ no longer holds

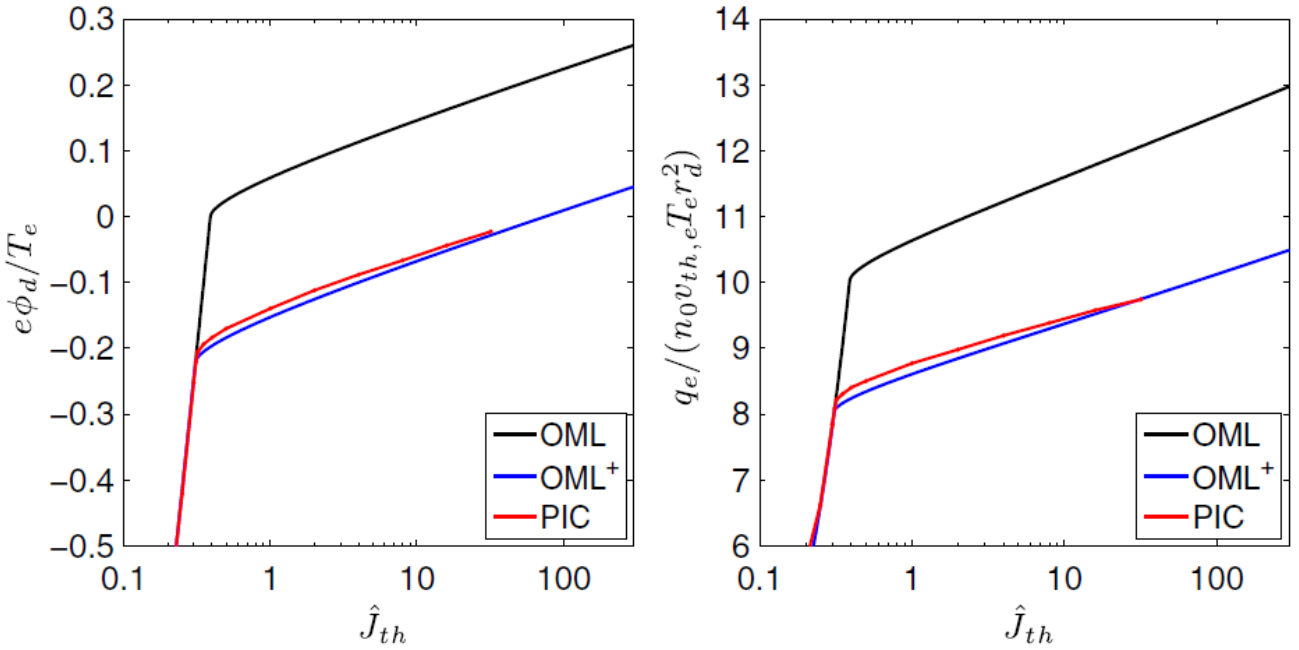

Strongly emitting dust

- Well known for the planar wall case: “space-charge limited sheath”, “virtual cathode”, “potential well” [Hobbs and Wesson, *Plasma Phys.* **9** 85 (1967); Takamura et al, *Contrib. Plasma Phys.* **44** 126 (2004)]

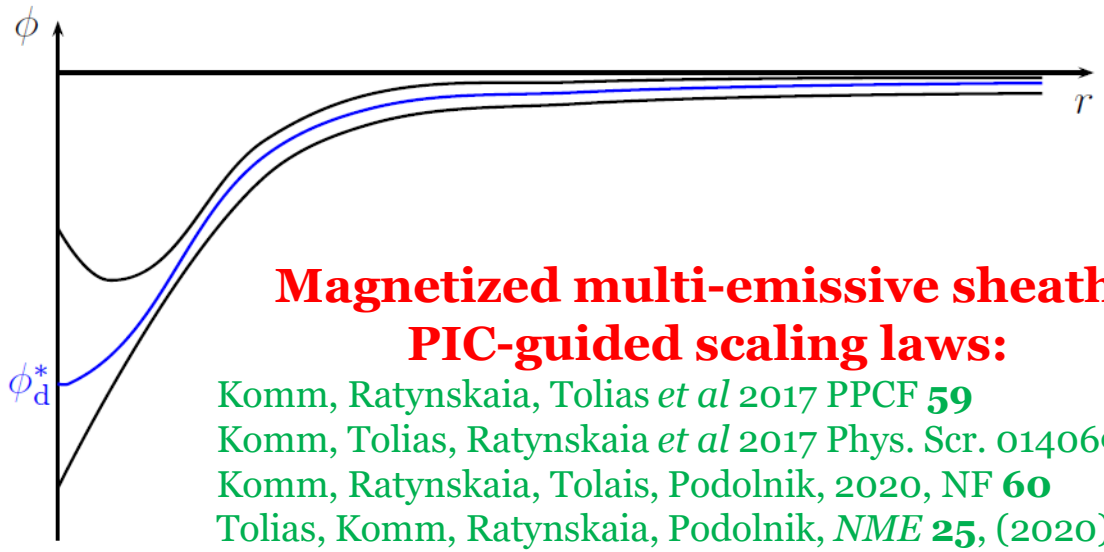

Magnetized multi-emissive sheaths PIC-guided scaling laws:

Komm, Ratynskaia, Tolias *et al* 2017 PPCF **59**
Komm, Tolias, Ratynskaia *et al* 2017 Phys. Scr. 014069
Komm, Ratynskaia, Tolais, Podolnik, 2020, NF **60**
Tolias, Komm, Ratynskaia, Podolnik, *NME* **25**, (2020)
Tolias, Komm, Ratynskaia, Podolnik, *NF* **63**, (2023)

Emitted electrons bring their own length scales into the problem. Strong emission of **cold electrons → small Debye length**

Strongly emitting grain [Delzanno & Tang, *PRL* **113** 035002 (2014)]

OML+ model:

- Corrections only when the dust is positively charged
- Knowing the critical dust potential ϕ_d^* is enough
- Modify the OML trapped-passing boundary condition for emitted electrons only

Relation $Q_d = 4\,\pi\,\varepsilon_0\,r_d\,\phi_d$ no longer holds

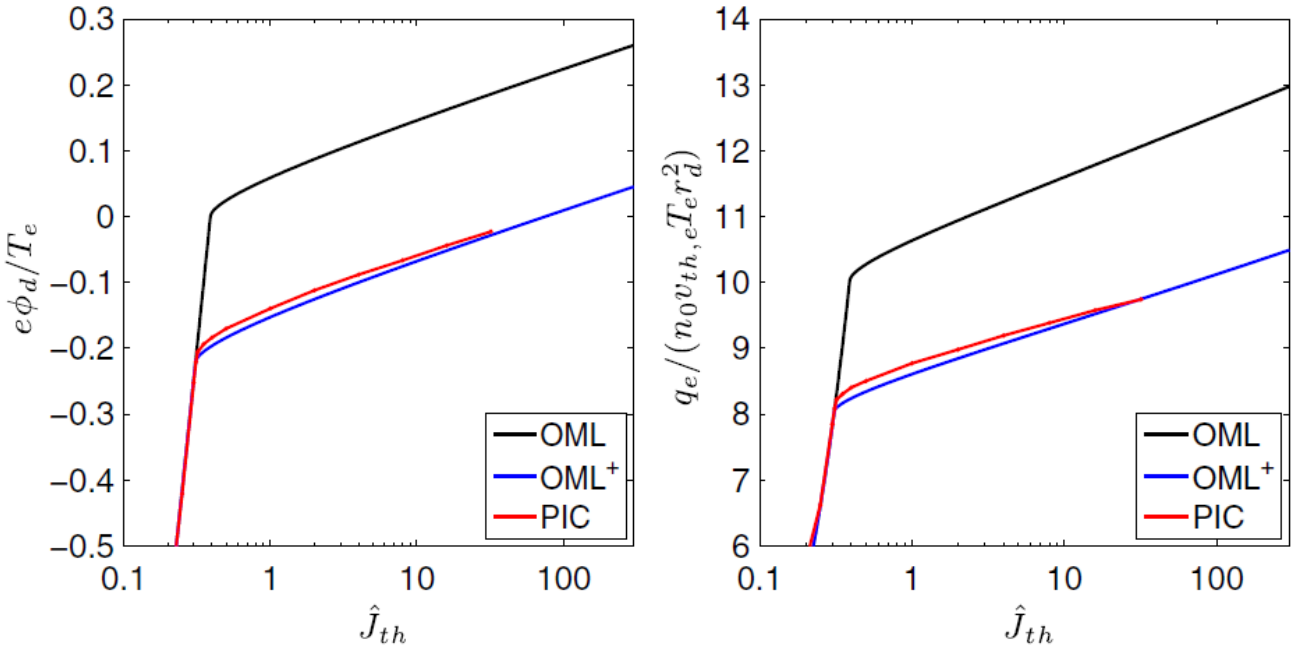

Chemical and kinetic contributions

Incident plasma fluxes Γ_i, Γ_e and emitted thermionic electron flux Γ_{th}

The kinetic components $q_{k,i}$ and $q_{k,e}$ depend on the dust potential

W_f is the work function

Incident ions : $$q_i = \Gamma_i \left(\sum_{j=1}^{Z} U_{iz}^{j} - Z\, W_f + U_{sb} \right) + q_{k,i}$$

Neutralization with the valance electrons

U_{iz} is ionization energy, Z is charge number, U_{sb} surface binding energy

Incident electrons: $$q_e = \Gamma_e\, W_f + q_{k,e}$$

Absorbed electrons equilibrate at the top of the valence band

Escaping thermionic electrons: $q_{te} = \Gamma_{th}(W_f + 2\, k_B T_s)$ surface cooling

Filling the thermal vacancy, assumed at the Fermi level

Importance of the magnetic field

- B fields in tokamaks are typically of several teslas (ITER baseline 5.3 T)

- Regimes of interest
  - Dense and cold divertor regions: $n_e \sim 10^{21}$ m^{-3}, $T_e \sim 1$ eV
  - Disruption scenarios with transient profiles

- Magnetized electrons: $R_\mathrm{d} \gg R_\mathrm{Le}, \lambda_\mathrm{De}$
- Ions generally unmagnetized or weakly magnetized, $\lambda_{De} \ll R_\mathrm{d} \lesssim R_\mathrm{Li}$

- Models addressing such regime exist for probes (Bohm 1949, Cohen 1960, Sanmartin 1970)→ adaptation to dust simulations Vignitchouk, Ratynskaia, Tolias *Plasma Physics Control. Fusion* **59** (2017)

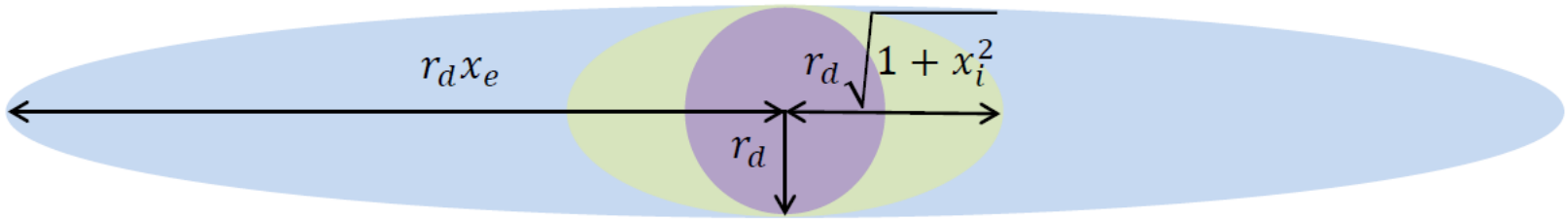

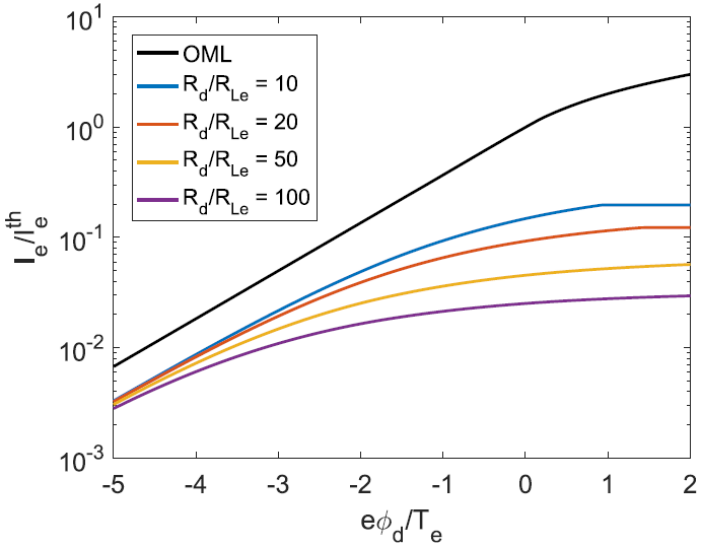

Microphysics of electron absorption

- Main parameters: $\lambda_{De} \approx 2$ µm, $R_d \approx 4$ µm, $R_{Le} \approx 6$ µm, $T_e \approx 2$ eV
- Direct measurements of the dust temperature via thermal radiation
- Statistically meaningful study of many (> 1000) measurements
- Conclusion: W_f contribution to electron heat flux is crucial for such cold plasmas (e.g. detached divertor)

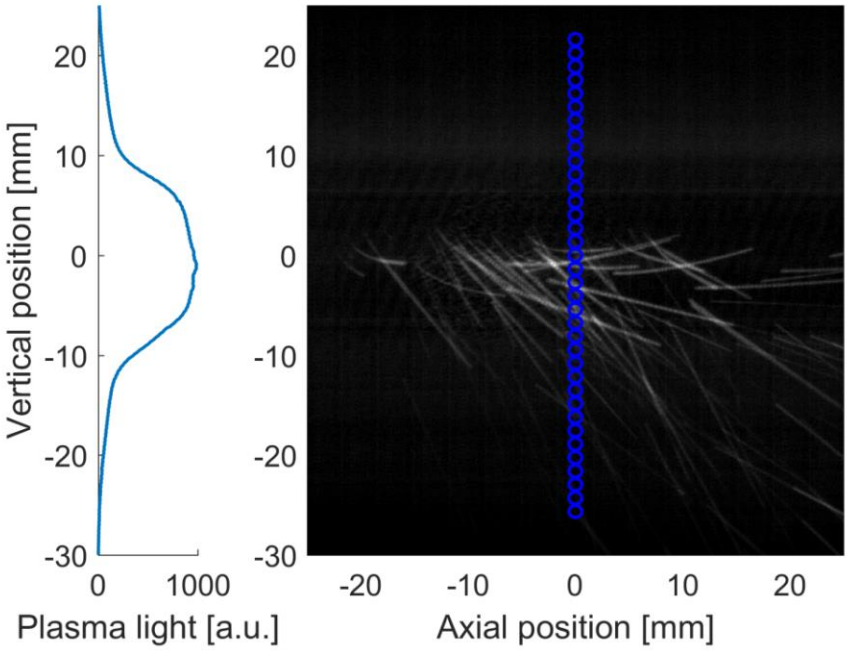

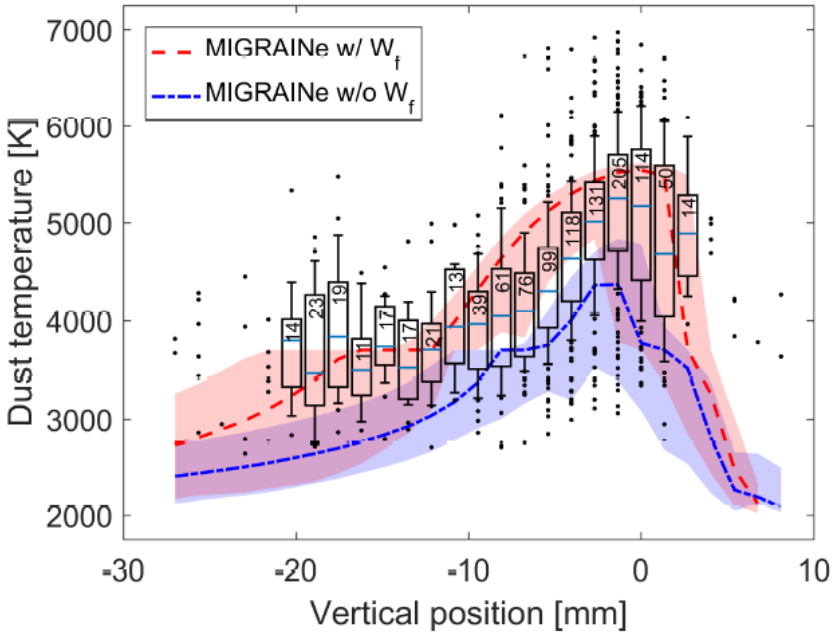

Vignitchouk, Ratynskaia, Kantor *et al*, *Plasma Physics Control. Fusion* **60** (2018)

Microphysics of ion absorption

EXAMPLE: Be droplets in disrupted plasmas

- Multiply charged Be ions present due to PSI
- Multiply charged Ne ions present due to MGI
- High ionization states persist after T_e drop (DINA simulations for ITER)
- Newly created Be droplets are generated and injected in this environment

	$Z_i = 1$	$Z_i = 2$	$Z_i = 3$	$Z_i = 4$	$Z_i = 5$
Be	9.3 eV	18.2 eV	153.9 eV	217.7 eV	-
Ne	21.6 eV	41.0 eV	63.4 eV	97.1 eV	126.2 eV

Implications for dust survivability in disrupted plasmas

$$Q_i \simeq q_{k,i} + \left(\sum_{j=1}^{Z_i} U_{iz}^{j} - Z_i W_f \right)$$

$\sum_{j=1}^{4} U_{iz}^{j}(\mathrm{Be}) \simeq 400$ eV for $\mathrm{Be}^{4+} \rightarrow$ 380 eV due to microphysics

$\sum_{j=1}^{5} U_{iz}^{j}(\mathrm{Ne}) \simeq 350$ eV for $\mathrm{Ne}^{5+} \rightarrow$ 325 eV due to microphysics

10-20% reduction of the contribution due to potential electron emission (Auger, autoionization) should be expected, the yields can exceed 5 but the average ejection energy is less than 10 eV.

These are extrapolations, no data available for multiply-charged ions on Be metals

Example:

Survival and in-vessel redistribution of Be droplets after ITER disruptions

Be dust production from transient melt events during ITER disruptions

- External input: disrupting plasma profiles and droplet injection points
- Assumptions: range and distribution of droplet sizes and speeds from theoretical estimates

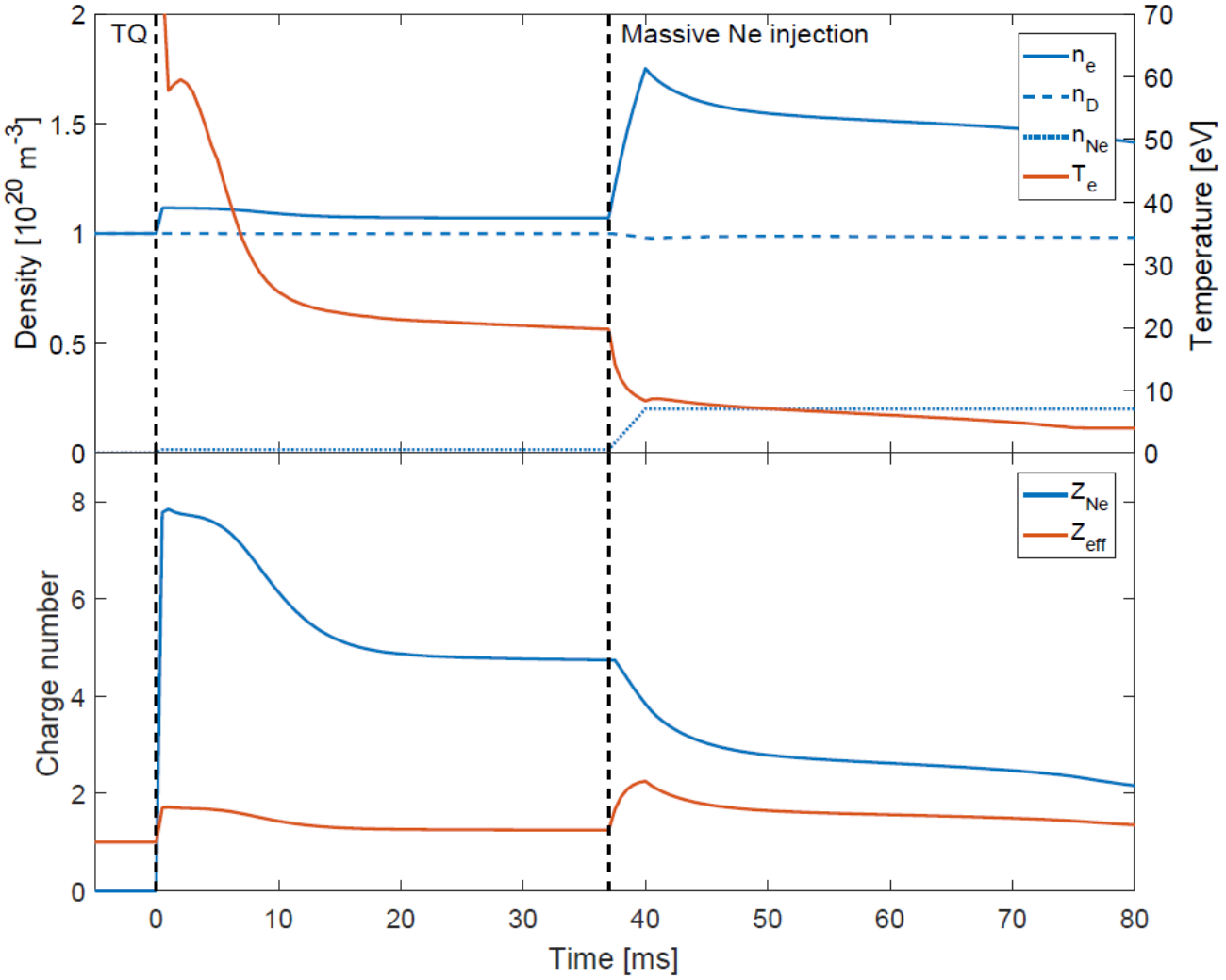

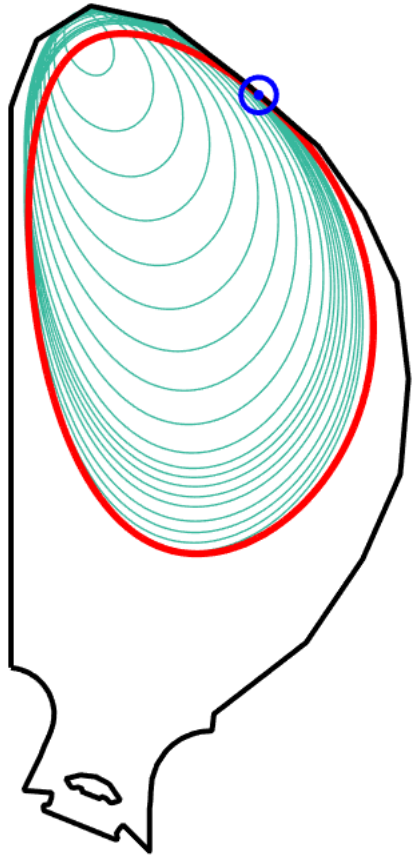

Vignitchouk, Ratynskaia, Tolias, Pitts *et al*, *Nuclear Fusion* **58** (2018)

Be dust production from transient melt events during ITER disruptions

MIGRAINe simulation output: droplet-to-dust conversion rates, identification of dust accumulation sites, size distribution of accumulated dust

	MD			VDE		
	Small	Medium	Large	Small	Medium	Large
Modal droplet radius (μm)	30	75	120	30	75	120
Vaporized mass (%)	40.2	26.7	18.3	88.5	67.9	50.1
Liquid mass (%)	56.5	71.3	80.7	10.9	31.0	49.2
Dust mass (%)	3.3	2.0	1.0	0.6	1.1	0.7
3 μm dust fraction (%)	26.1	11.9	0.5	48.6	23.3	3.1
2nd modal dust radius (μm)	17	65	105			

Low conversion efficiency into solid dust

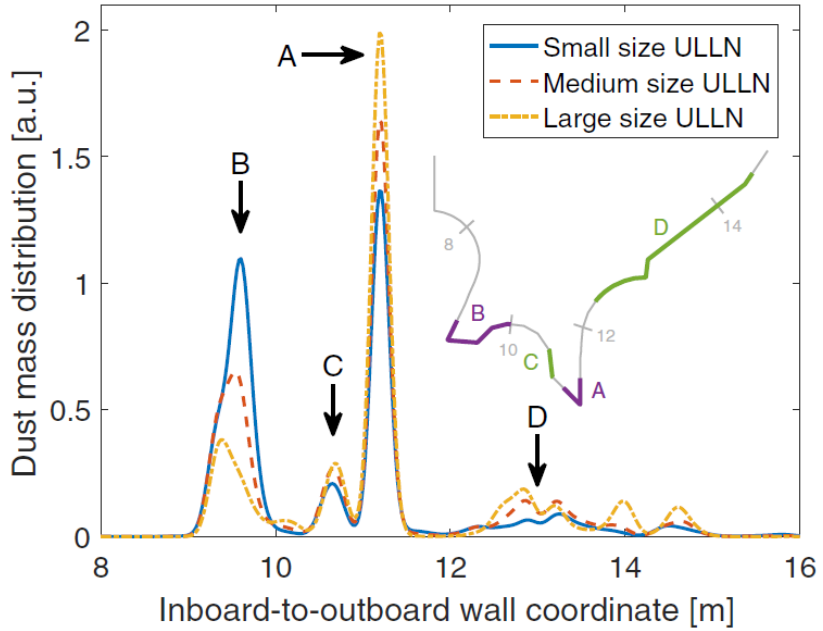

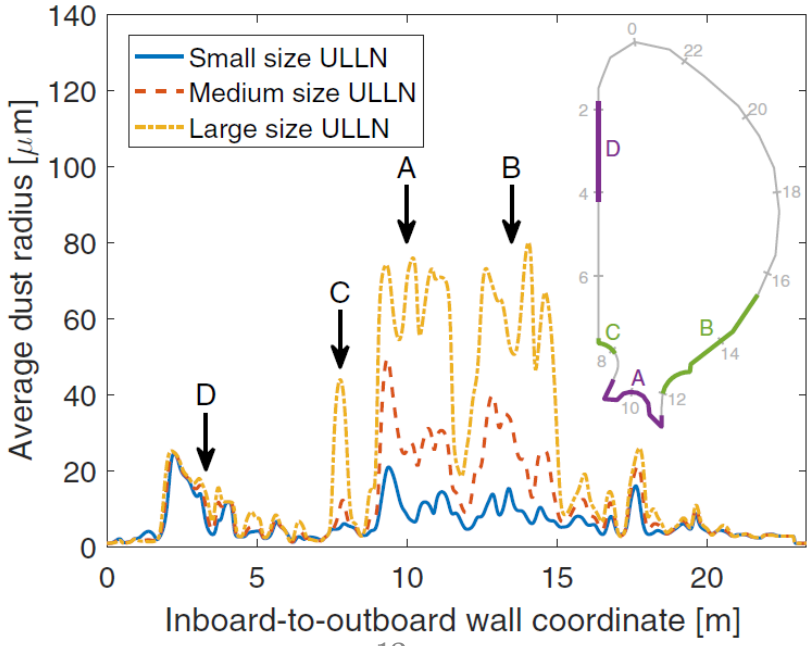

Adhesion, remobilization and dust-wall collisions

Mechanical impacts

Newton's 2d law

$$M_d\,\ddot{\alpha} + P = 0$$

- The contact radius a
- The relative approach α
- The contact force P

(chosen positive when compressed and the force tends to separate the bodies)

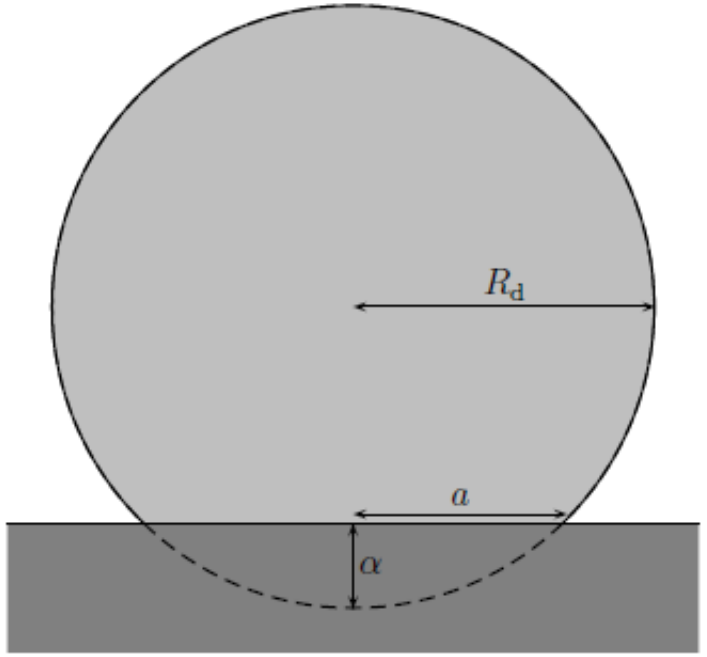

Simplified visualization of a sphere-plane contact

The energy budget of the impact is given by

$$\frac{1}{2}M_d\,\dot{\alpha}^2 + \int^{\alpha} P(\alpha')d\alpha' = 0$$

Compressive work $W(\alpha)$ by the contact forces from the contact initiation to the current time

Elastic impacts (Herz's theory) + dissipative effects (plasticity and adhesion)

Mechanical impacts: force – displacement diagrams

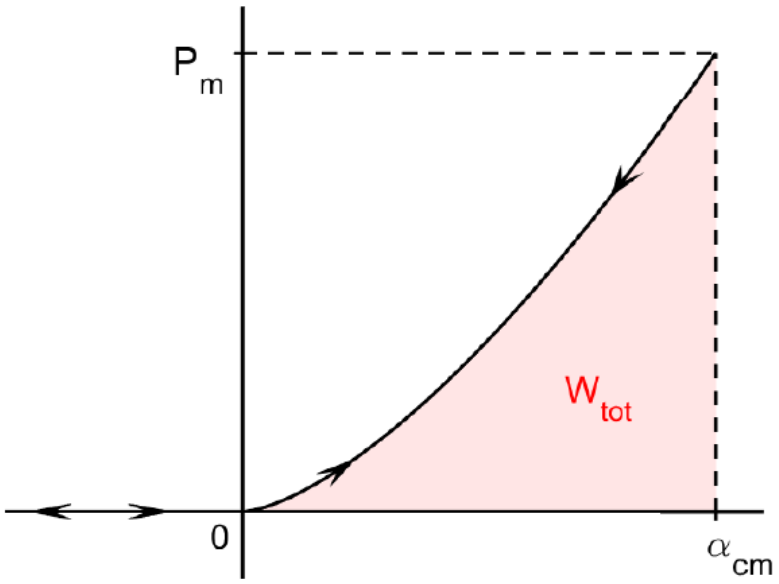

Normal Hertzian elastic impact

The shaded area W_{tot} represents the total compression work done during the impact, which is equal to the sphere's initial kinetic energy $W_0 = W_{tot}$

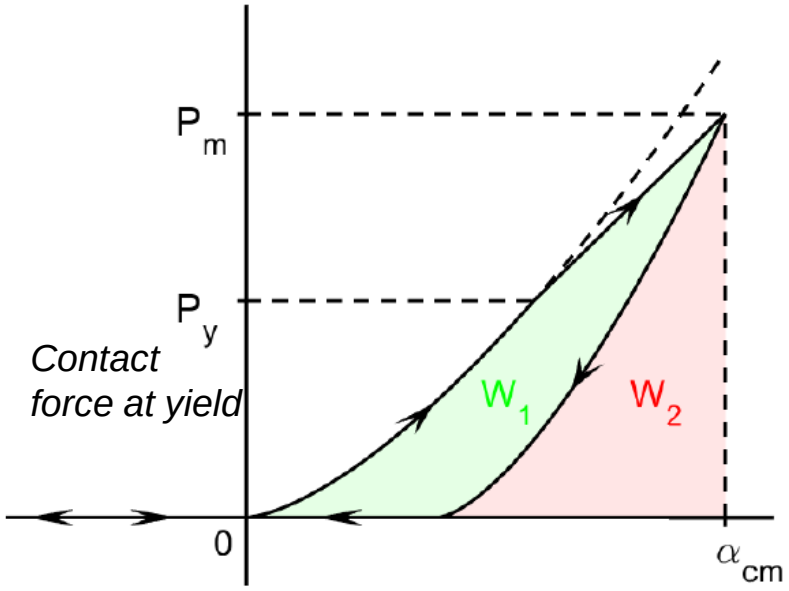

Normal elastic-plastic impact

Plastic deformations are initiated at a contact force threshold P_y.
Out of the initial kinetic energy $W_0 = W_1 + W_2$ of the sphere, W_2 is recovered after the impact while W_1 is dissipated into irreversible deformations.

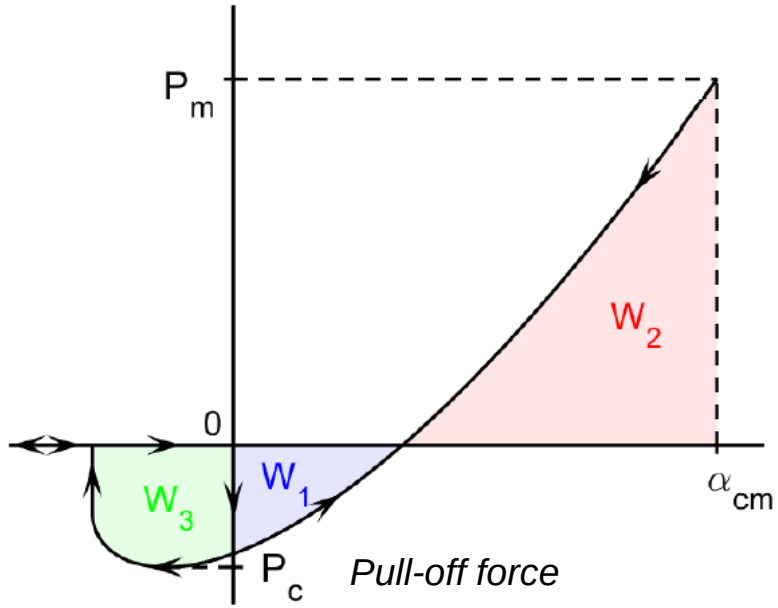

Normal elastic-adhesive impact

JKR theory [Johnson, Kendall and Roberts, Proc. R. Soc. A 324 (1971) 301]

Initial energy $W_0 = W_2 - W_1$
The energy W_3 is dissipated to detach the surfaces at the end of the impact, rebound energy $W_0 - W_3$

Main quantities of interest : normal impacts

Adhesive velocity v_s^{adh} in elastic-adhesive impacts (Newton's equation+ JKR theory)
Johnson, Kendall, Roberts, *Proc. R. Soc. A* **324** (1971) 301)

$$v_s^{adh} = \frac{\sqrt{3}}{2}\pi^{1/3}\sqrt{\frac{1+6\times 2^{2/3}}{5}}\left(\frac{\Gamma^5}{\rho_d^3 E^{*2} R_d^5}\right)^{1/6} \simeq \text{few m/s}$$

ρ_d , R_d are dust mass density, radius, E^* the reduced Young modulus, Γ the interface energy
For $v_i^{\perp} \le v_s^{adh}$ adhesion forces make grain stuck to the surface, while
for $v_i^{\perp} > v_s^{adh}$ collision is inelastic owing to the irreversible work $\frac{1}{2} m_d \, (v_s^{adh})^2$

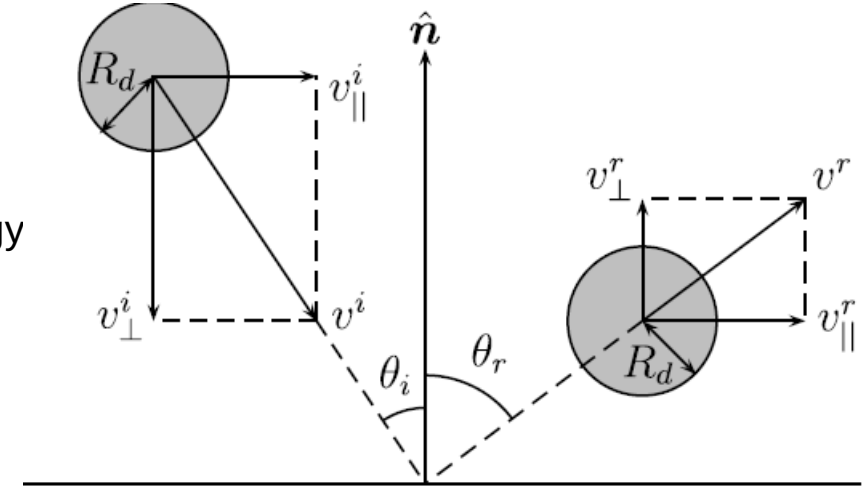

Yield velocity $v_y = \frac{\pi^2}{2\sqrt{10}}\left(\frac{p_y^5}{\rho_d \, E_{*4}}\right)^{1/2}$ in elastic-perfectly plastic impacts

p_y is limiting contact pressure, typically $1.6 - 2.8\ \sigma_y$, where σ_y is the yield strength
For $v_i^{\perp} > v_y$ dust impact energy is enough to cause plastic deformation, while
for $v_i^{\perp} \le v_y$ the collision is totally elastic *when ignoring adhesion*

Basic picture:

- gradual reduction of normal velocity → value below the adhesive velocity → dust is adhered to the wall
- Size selectivity; smaller dust stucks easier, larger dust under more collisions

- Outcome of collision can be predicted by restitution coefficients $e_\perp$ (rebound to incident speed ratio) the normal impact of elastic–perfectly plastic adhesive spheres [Thornton C. and Ning Z. 1998 *Powder Technol.* **99** 154], $e_\perp$ function of $v_i^{\perp}$, v_s^{adh} and v_y

Validation in plasma environments (Pilot-PSI)

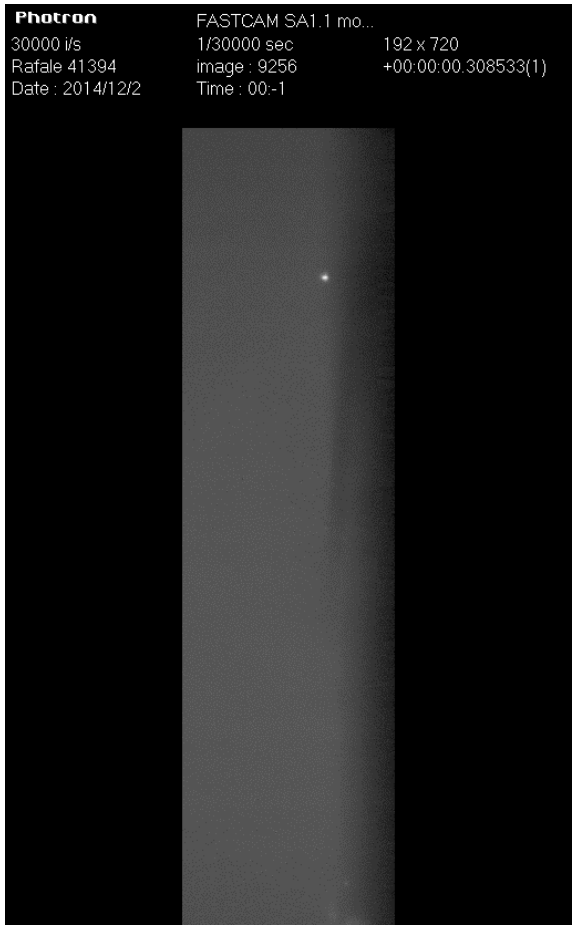

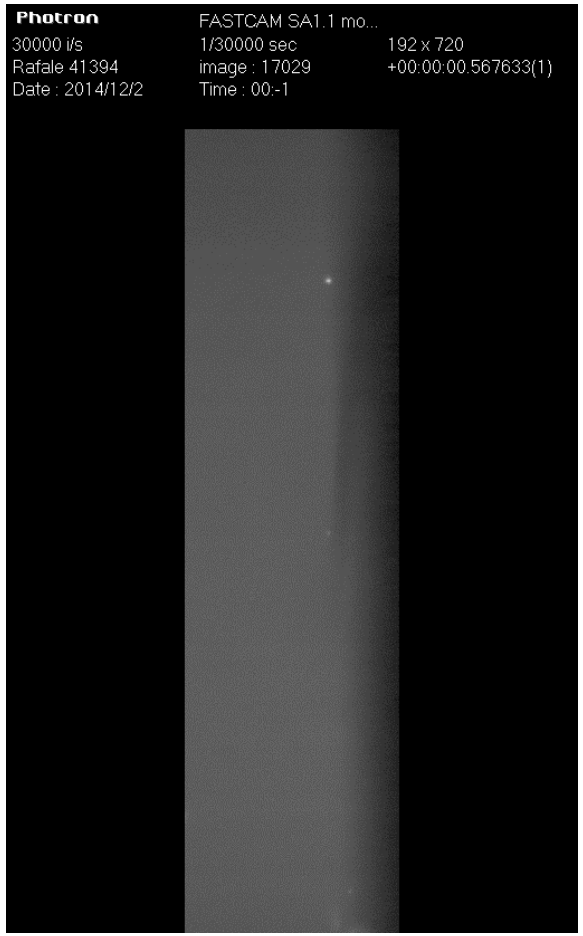

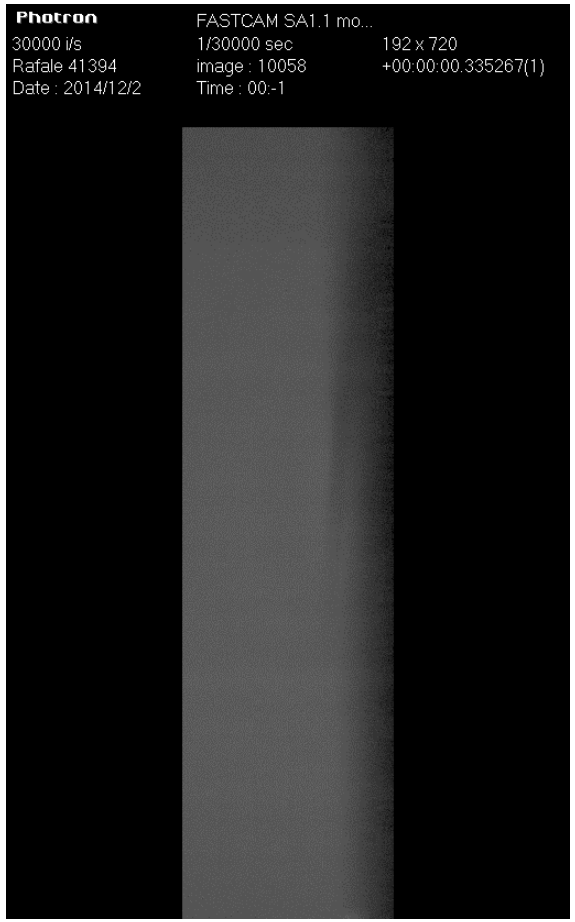

Ratynskaia *et al*, *JNM* **463** 877 (2015)
Shalpegin *et al*, *NF* **55** 112001 (2015)
Tolias *et al*, *NME* **12** 524 (2017)

Validation in plasma environments (Pilot-PSI)

Spatial resolution down to 6.5 μm/pixel achieved in Pilot-PSI (spherical 5-25μm W dust) NF 55 (2015) 112001

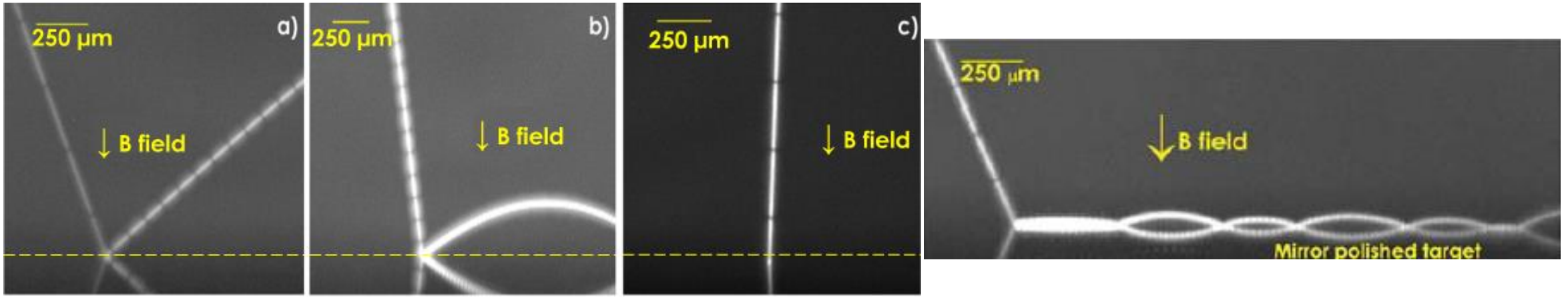

(a) *small loss of normal velocity,* $e_{\perp}= 0.7$, $e_{||}= 0.95$; ***(b)*** *substantial loss,* $e_{\perp}= 0.2$, $e_{||}= 1$; ***(c)*** *sticking ;* ***(d)*** *multi-bouncing*

Plasma not relevant for instantaneous impacts

- Dissipation of $v\perp$ due to adhesive and plastic losses & nearly preserved v || (frictionless contact)
  - No rebound when **(i)** normal velocity < sticking value **(ii)** High temperature

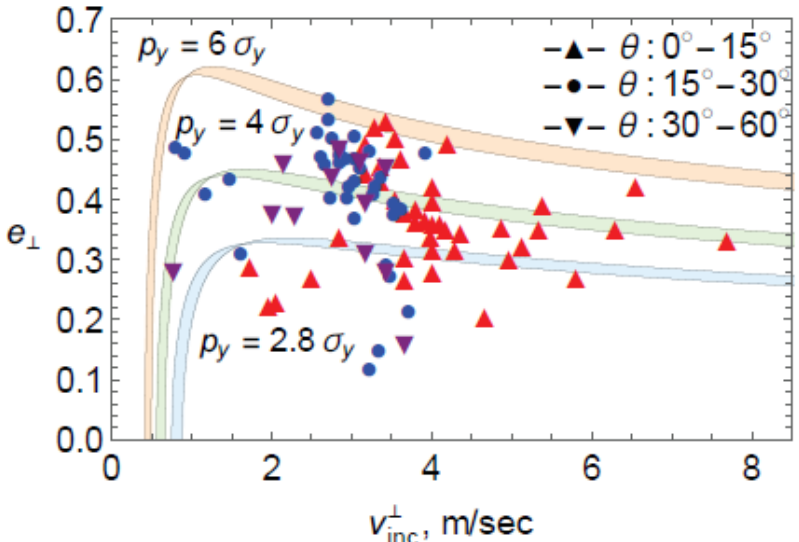

Thornton and Ning approach, elastic-perfectly plastic adhesive spheres Powder Technol. 99 (1998)

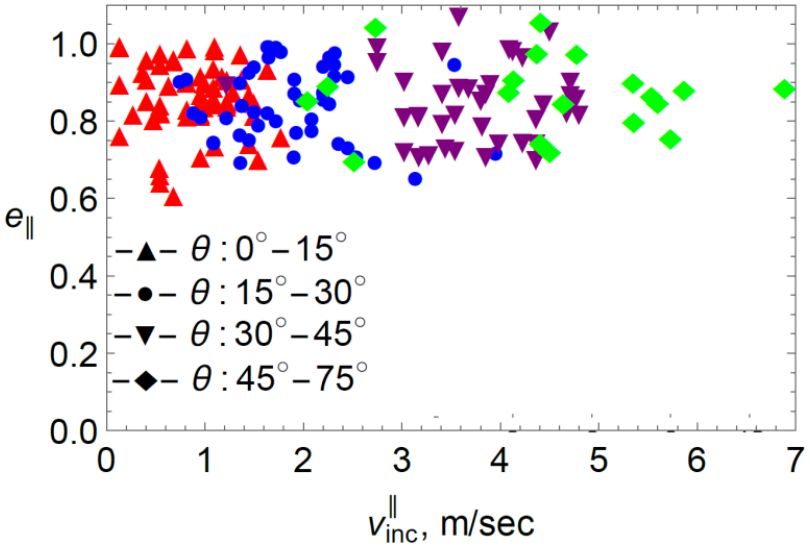

Be dust production during ITER disruptions

Output: droplet-to-dust conversion rates, identification of dust accumulation sites, size distribution of accumulated dust

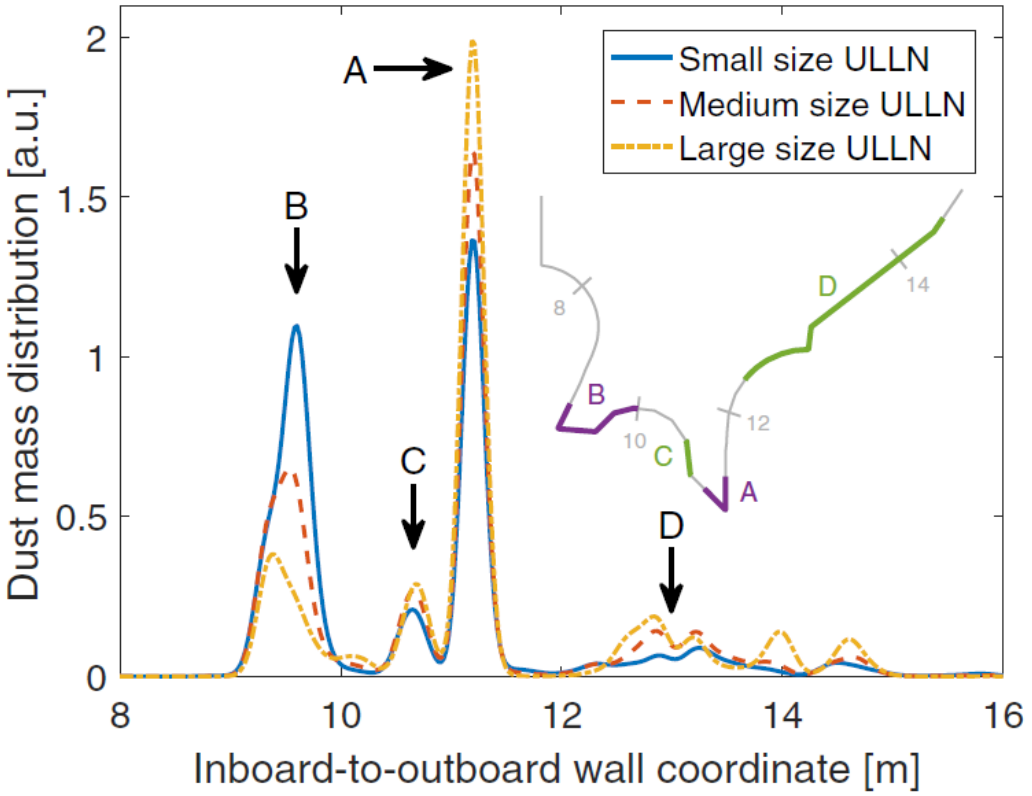

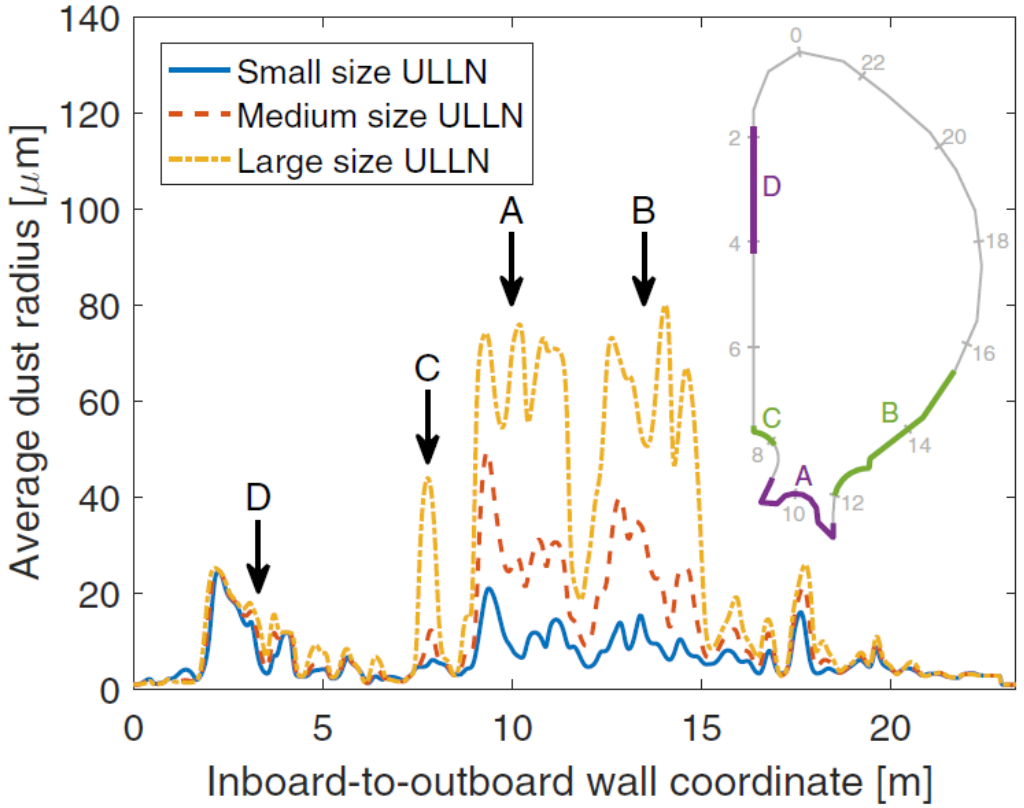

Main quantities of interest : remobilization under steady-state

- Multiple collisions of dust with the wall → gradual reduction of normal velocity → value below the adhesive velocity → dust is adhered to the wall

- Plasma forces can remobilize dust but they need to overcome adhesion.

- Pull-off force minimum normal force to separate two bodies (in the JKR model):

$$|F_{\mathrm{a}}| = \left|F_{\mathrm{po}}\right| = 3\pi\Gamma R_d/2 \quad \propto R_d$$

- *For smooth surface:* Plasma forces ($\propto R_{\mathrm{d}}^2$) and gravity ($\propto R_{\mathrm{d}}^3$) cannot detach 10 μm sized W dust, for ITER divertor parameters

$$F_{po} \sim 10^2 F_{id}^{sc} \sim 10^3 F_{id}^{abs} \sim 10^3 F_E^{***} \sim 10^6 F_g$$

Tolias, Ratynskaia, De Angeli *et al, PPCF* **56** 123002 (2016)

- Size scalings suggest that larger dust or agglomerates can remobilize more easily

*** The contact charge for spherical conducting grain lying on conducting plane in the presence of uniform E field [Lebedev and Skalskaya 1962]

Validation in plasma environments- cross-machine study

Tolias *et al,* PPCF **56** (2016) ; Ratynskaia *et al,* NME **12** 569 (2017)

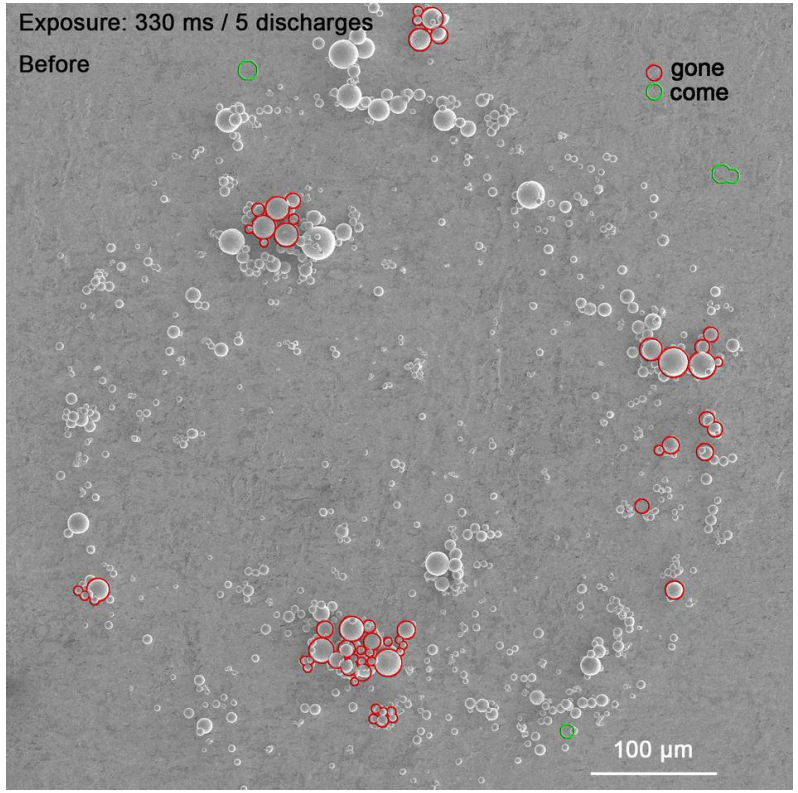

EXTRAP T2R

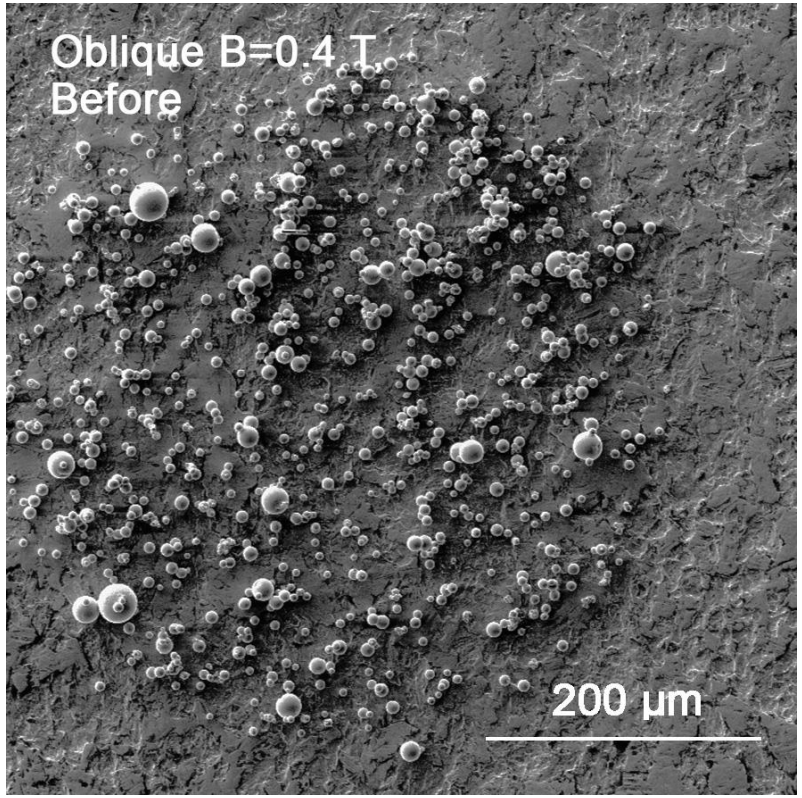

Pilot-PSI oblique

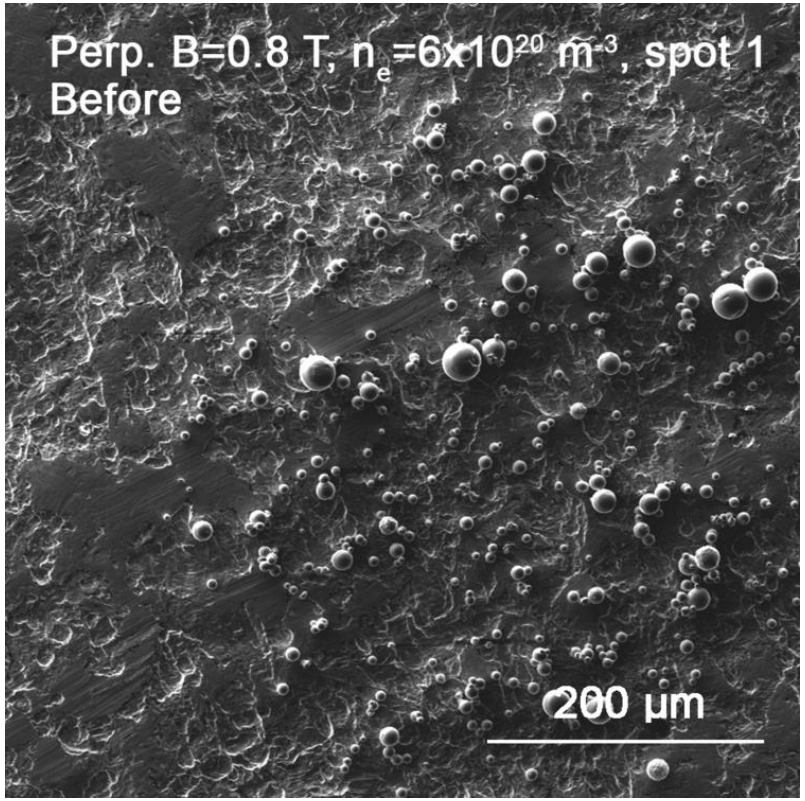

Pilot-PSI normal

Validation in plasma environments- cross-machine study

Cross-machine study: W-on-W exposures in linear devices, reverse field pinches, tokamaks.

Tolias *et al,* PPCF **56** (2016) ; Ratynskaia *et al,* NME **12** 569 (2017)

- Similar results despite the strong variation of the plasma parameters.
- *On average,* large dust grains ($\gtrsim 10\mu$m) and agglomerates remobilize much more easily, as expected from simple scalings → smaller dust expected to reside on PFCs.
- Overall dust remobilization rate is higher than estimated.

Overlaid SEM prior – post exposure to ***Pilot-PSI***

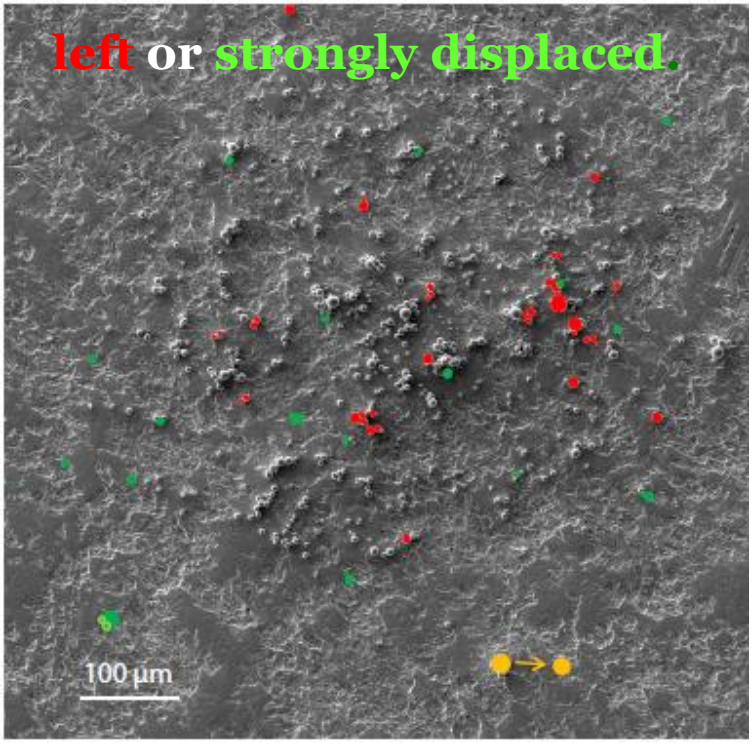

Direct lift-up condition:

$$F_i^n + F_E > F_p$$

Adhesion is weaker than JKR predictions?

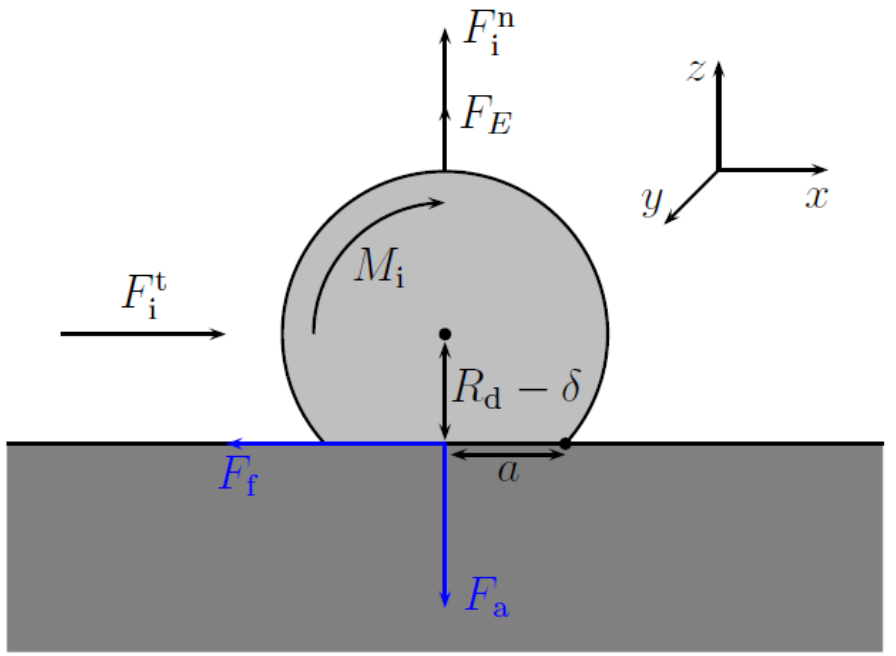

Sliding condition: $F_i^t > \mu_s(F_p - F_i^n - F_E)$

Depends on static friction coefficient value

Rolling condition: $M_i + F_i^t(R_d - \delta) > a\,(F_p - F_i^n - F_E)$

In the typical small deformation limit $R_d \gg a,\ \delta$

G. M. Burdick, *et al.*, J. Nanopart. Res. 3 (2001) 455
M. A. Hubbe Colloids Surf. 12 (1984) 151

W-on-W adhesion: measurements

First measurements of W-on-W adhesion with *electrostatic detachment method* for spherical monodisperse μm W dust (high purity, no porosity, excellent conductivity) Riva *et al*, *NME* **12** 593 (2017)
Similar results by other groups with AFM Peillon *et al, J. Aerosol Sci.* **137** (2019)

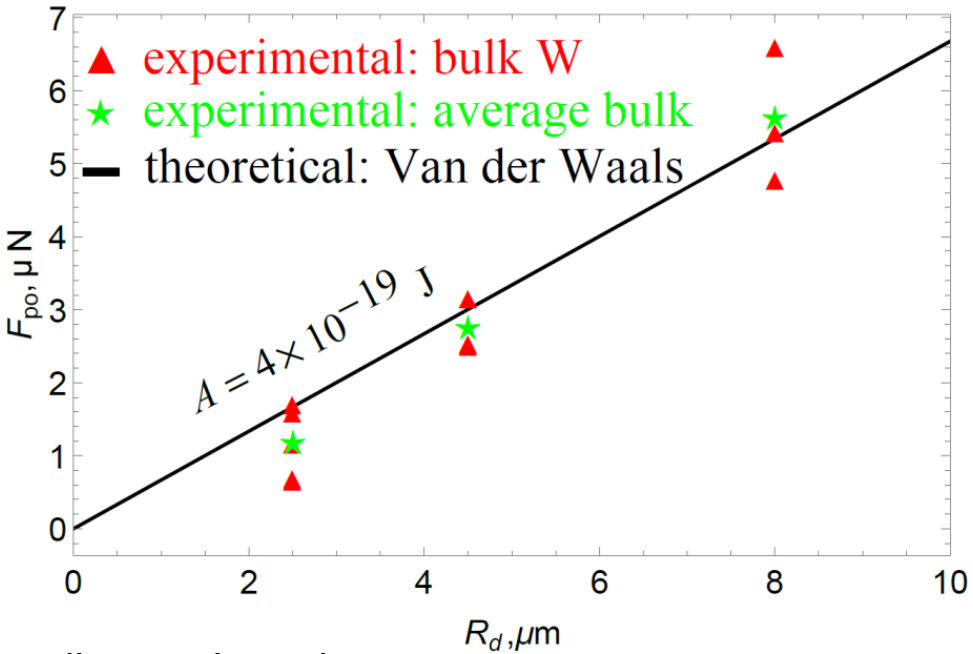

- The measurements: contact mechanics models (JKR, DMT) overestimate the adhesion force by ~ 2 orders of magnitude. The standard van der Waals expression agrees well with experiments.
- Contact mechanics models implicitly assume that *extremely short range strong metallic forces* generate adhesion, van der Waals models explicitly assume that *long range weak induced multipole interactions* generate adhesion.
- Metallic bonding results from electron exchange interactions characterized by extremely short range and negligible beyond 1nm.
- **Surface roughness ~ of few nm suffices to switch the dominant contact force from metallic bonding to van der Waals attraction →** dramatic decrease of surface energy
- Tokamak relevant heat treatments below the W recrystallization range lead to increase of the W-on-W adhesion force up to two orders of magnitude irrespective of the dust size Tolias *et al, MNE* **24** 100765 (2020)

W-on-W adhesion versus gravity

Let us consider the scenario of **weakest** adhesion that corresponds to rough contaminated surfaces and very low speed dust deposition. Based on the experimental results, this implies a retarded Hamaker constant $A \simeq 10^{-19}\mathrm{J}$ and a distance of closest approach $z_0 \simeq 0.4\mathrm{nm}$ with the adhesion force given by

$$F_{\mathrm{adh}} = \frac{A}{6z_0^2} R_{\mathrm{d}}$$

The ratio of the adhesion force over the gravity scales as $F_{\mathrm{adh}}/F_{\mathrm{g}} \propto 1/R_d^2$, which immediately reveals that gravity becomes negligible for small dust grains.

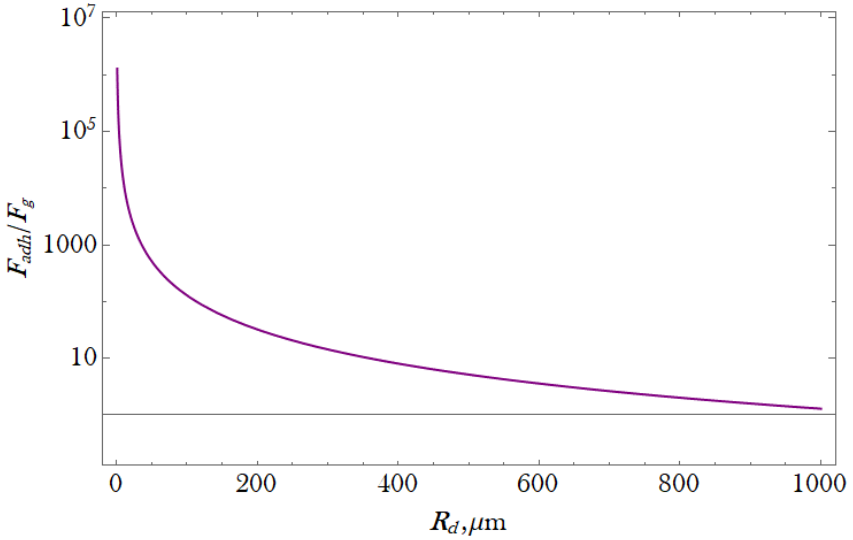

Gravity becomes comparable to adhesion only for dust radii larger than 1mm!

W-dust adhered on a planar W substrate (Pilot-PSI campaign).

Dummy sample that was only mounted at the endplate but not exposed to the linear plasma. In the figure gravity was directed downwards along the vertical

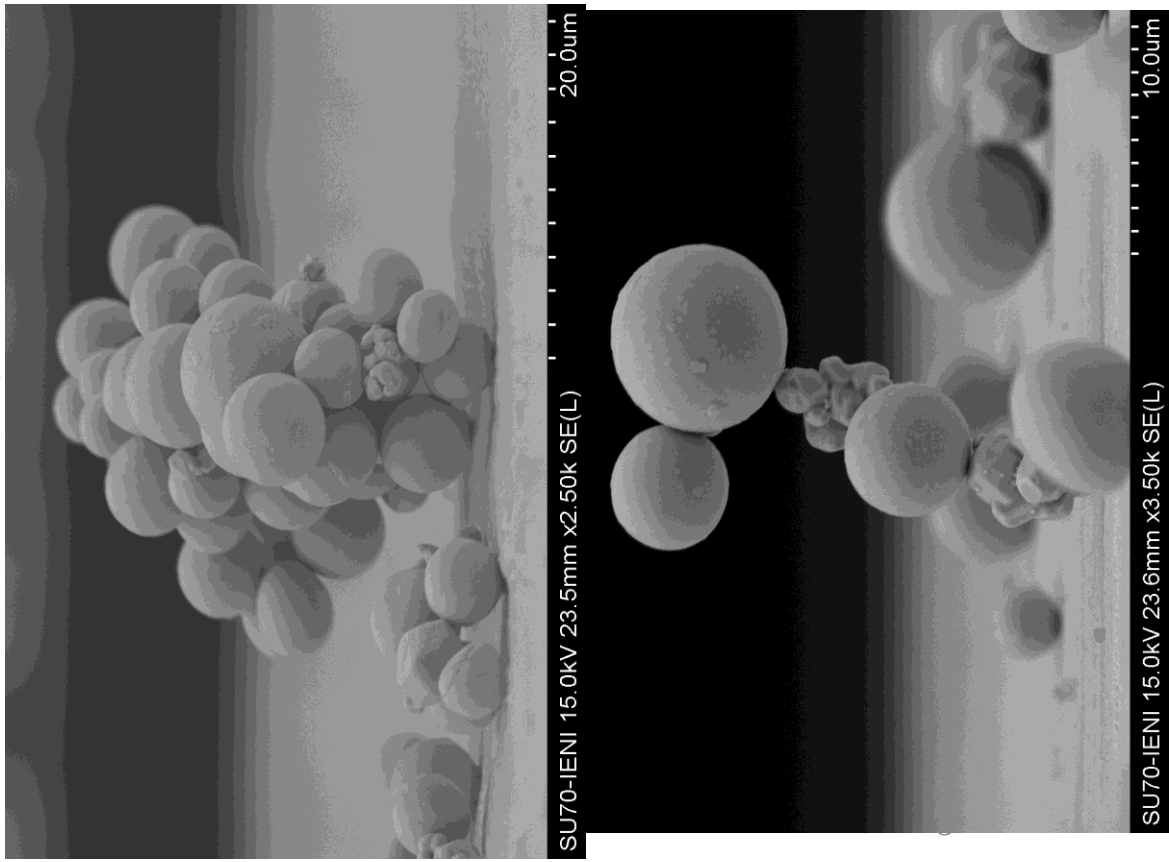

Remobilization under ELM-like heat loads: general picture

Do all grains melt or only those exhibiting macro-morphological changes (coalescence, spreading)?

- Clusters and agglomerates can melt much easier than isolated grains: physical connection of top grains to cooler substrate through bottom grains → smallness of contact area and the low thermal contact conductance imply poorer heat conduction

- Wetting induced coagulation: top grains receive most of incident heat flux and melt → bottom grains shadowed from incident heat flux, receive less through conduction, remain solid → top molten grains wet the bottom solid grains → larger dust

Why do the molten clusters remain or even tend to be spherical?

- Liquid metals excellent wettability on their own solids: $\theta_Y \ll 90^o$ in TE → spherical W droplets under ELMs, $\theta_{inst} \gg 90^o$ → they spread on bottom solid dust or W substrate → perfect sphere-on-sphere wetting leads to sphere, perfect sphere-on-plane to film

- Spreading dynamics driven by surface tension, limited by viscous dissipation: spreading vs resolidification rates → latter very fast due to short ELM duration, in inter-ELM periods dust grains resolidify as spheres not enough time to spread on PFC!

Remobilization under ELM-like heat loads: general picture

No observation of melting of isolated dust grains: despite large statistics
Recurring evidence of top-bottom wetting: especially for monodisperse dust

Strong interplay between wetting and resolidification (short ELM duration): Spreading dynamics do not fully evolve, signature capillary waves frozen by resolidification

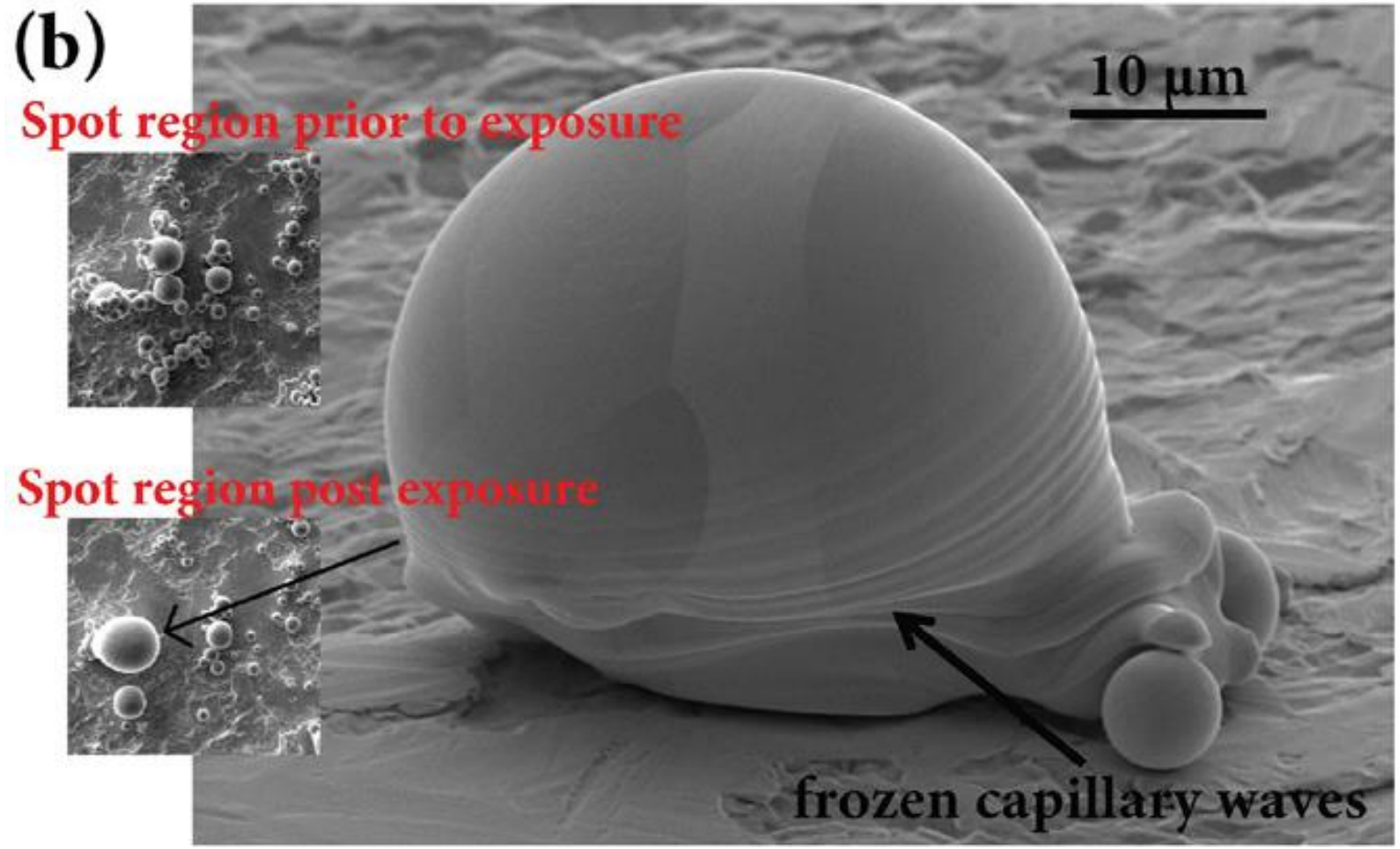

Ratynskaia et al, Nucl. Fusion **56** (2016) 066010

Summary

Modelling of metal dust–plasma & dust–wall interactions is genuinely inter-disciplinary as, in addition to plasma physics, it involves electron emission physics, impact mechanics, condensed matter physics & contact mechanics.

- ITER licensing imposes in-vessel inventory limits
- Modelling of droplet survival: heat budget and *initial release conditions* (inertia dominated dynamics)
- Numerical tools available (e.g. MIGRAINe dust dynamics code with all relevant surface physics and dust-wall collisions) for evaluating self-consistently momentum and energy transfer from plasma particles to the dust

- Droplet release: sizes & speeds depend on the mechanism (PFC melting under fast transients, RE, arcing, …)

- Contact mechanics model for dust-vessel collisions work well as plasma is not relevant for instantaneous impacts → Formation of accumulation sites can be predicted reliably

- Adhesion/remobilization modelling can be guided by contact mechanics models *but peculiarities* of fusion relevant surfaces and plasma effects make extra complications (surface roughness, increased temperatures) →

Remobilization of pre-existing dust

- under ramp-up/steady-state plasmas: lift-up only above a threshold size
- under ELMs: contact strengthening due to increased temperature → inhibited remobilization + formation of larger droplets by wetting-induced coagulation

Aspects not discussed in this presentation

- Non-ideal effects on adhesion: impurity films, atmospheric contaminants, surface roughness, heating
- Non-plasma induced remobilization:
  - magnetic moment force (for magnetic dust)
  - vibrational de-attachment
  - hydrodynamic mechanisms (in presence of gas/air flow)
- Rotational dynamics: spinning droplet (inertia vs surface tension) and spinning dust (inertia vs yield force) destruction
- Fuel retention → Oxidized tritiated tungsten dust may behave like dielectrics and sustain charge due to β-decay

For an exhaustive overview of dust in nuclear fusion reactors and present day machines see

Dust and powder in fusion plasmas: recent developments in theory, modeling, and experiments, S. Ratynskaia, A. Bortolon, S. I. Krasheninnikov, Reviews of Modern Plasma Physics 6, 20 (2022)

Modelling of dust generation, transport and remobilization in full-metal fusion reactors, S Ratynskaia, L Vignitchouk and P Tolias, Plasma Phys. Control. Fusion 64 044004 (2022)

Extra slides

Surface processes

Electron-induced electron emission

Electron-induced electron emission (EIEE)

- The impact of an electron stream on the surface of a bulk material is typically accompanied by the re-emergence of several electrons that can be categorized into different groups according to their generation process. Each group is quantified by its respective yield or coefficient.

- In terms of particle and energy fluxes, the most important groups are
  - *Secondary electrons*, *i.e.* emitted electrons that were initially bound to the material prior to their excitation by the incident electrons (quantified by the secondary electron emission yield δ)
  - *Backscattered electrons*, *i.e.* incident electrons that were in-elastically reflected from the interior of the material after their penetration (quantified by the electron backscattering yield η)
  - *Reflected electrons*, *i.e.* incident electrons that were quasi-elastically reflected by the potential barrier located at the ambient-material interface (quantified by the electron reflection coefficient R)

- The total electron-induced electron emission yield is an additive quantity that is given by

$$\sigma = \delta + \eta + R$$

  - *For very low incident energies*, quasi-elastic electron reflection is dominant.
  - *For low and intermediate incident energies*, secondary electron emission is dominant.
  - *For high incident energies*, electron backscattering is dominant.

Energy transfer in EIEE

- *In absence of electron emission*, an incident electron of energy E_{inc} that is impinging on a metal target will gradually lose its energy in inelastic collisions with the valence and core electrons of the target.
- Ultimately, it will accommodate at the top of the valence band after it thermalizes with the metal and acquires a kinetic energy $\left(\frac{3}{2}\right) k_{\mathrm{B}} T_{\mathrm{m}}$ → the energy transferred to the target is $E_{\mathrm{inc}} - (3/2) k_{\mathrm{B}} T_{\mathrm{m}}$
- However, the electron is no longer free but it is bound to the metal with a binding energy that is equal to minus the work function W_{f}.

$$Q_{\mathrm{e}} = E_{\mathrm{inc}} - \frac{3}{2} k_{\mathrm{B}} T_{\mathrm{m}} + W_{\mathrm{f}}$$

- *In the presence of electron emission,* the average exit energies of the emitted electrons need to be subtracted together with the binding energy contribution. Introducing a cooling term

$$-Q_{\mathrm{c}} = \delta \bar{E}_{\mathrm{SEE}} + \eta \bar{E}_{\mathrm{EBS}} + R \bar{E}_{\mathrm{QER}} - \sigma \frac{3}{2} k_{\mathrm{B}} T_{\mathrm{m}} + \sigma W_{\mathrm{f}}$$

where $\sigma = \delta + \eta + R$ for the total EIEE yield.

$$\bar{E}_{\mathrm{SEE}} = 2W_{\mathrm{f}} \quad \bar{E}_{\mathrm{EBS}} \simeq 0.6 E_{\mathrm{inc}} \quad \bar{E}_{\mathrm{QER}} \sim E_{\mathrm{inc}}$$

Surface processes

Ion-induced electron emission

Ion surface neutralization

- Relatively low energy (sub-keV) singly charged ions that are present in the Ångström vicinity of metal surfaces are neutralized in a very effective manner owing to the relative large interaction times and the valence electron availability for tunneling.
- Systematic ion beam experiments confirmed that neutralization probability approaches 100% at sub-keV energies.

- Surfaces get positively charged when absorbing ions, because they lose negative charge for the ion neutralization and not because they directly gain positive charge.
- Owing to the very high neutralization probability, ion backscattering and ion sputtering do not constitute charging mechanisms in contrast to electron backscattering

- Ion neutralization can take place as a result of one of the following electron transfer mechanisms:
  - resonant transitions involving one valence electron
  - Auger transitions involving two valence electrons
  - combinations of resonant and Auger transitions
  - radiative transitions involving one valence electron (highly improbable for sub-keV incident energies)
  - quasi-molecular transitions involving one core metal electron (highly improbable for sub-keV incident energies)

Ion-induced electron emission (IIEE)

- The impact of an ion stream on the surface of a bulk material is typically accompanied by the re-emergence of several electrons that can be categorized into different groups according to their generation process. Each group is quantified by its respective yield

- In terms of particle and energy fluxes, the most important processes are
  - *Ion induced potential electron emission*, a pure surface phenomenon where the energy required for the bound electron excitation and subsequent ejection is provided by the internal energy stored in the ions that is released when they are neutralized at the surface (quantified by the yield γ_{p})

  - *Ion induced kinetic electron emission*, a nominally volume phenomenon, where the energy required for the bound electron excitation and subsequent ejection is provided by the kinetic energy carried by the ions that is released during their inelastic collisions with the bound electrons (quantified by the on yield γ_{k})

- The total ion-induced electron emission yield is an additive quantity that is given by

$$\gamma = \gamma_{\mathrm{k}} + \gamma_{\mathrm{p}}$$

  - For very low incident energies, there is no kinetic electron emission.
  - For very high incident energies, there is no potential electron emission.
  - For certain ion / target combinations, there is no potential electron emission regardless of the incident energy.

Energy transfer in neutralization and IIEE

- *In absence of electron emission, ion backscattering, sputtering*: a **singly charged ion** of energy E_{inc} impinging on a metal target will be first neutralized, then gradually lose its energy in inelastic collisions with electrons or elastic collisions with nuclei and finally accommodate at the surface. Three contributions to the energy transferred to the target:
  - ✓ Kinetic contribution equal to the difference between the incident ion energy and the thermal energy, $E_{\mathrm{inc}} - (3/2)k_{\mathrm{B}}T_{\mathrm{m}}$
  - ✓ Neutralization contribution equal to the difference between the electron binding energies that are the ionization energy and work function (irrespective of neutralization process, the electron hole will reach the valence band top in equilibrium), $U_{\mathrm{iz}} - W_{\mathrm{f}}$
  - ✓ Accommodation contribution equal to the surface binding energy, U_{sb}

$$Q_{\mathrm{i}} = \left(E_{\mathrm{inc}} - \frac{3}{2}k_{\mathrm{B}}T_{\mathrm{m}}\right) + (U_{\mathrm{iz}} - W_{\mathrm{f}}) + U_{\mathrm{sb}}$$

- *In absence of electron emission, ion backscattering, sputtering*: a **multiply charged ion** of energy E_{inc} will follow the same path, but the neutralizations will be multiple. Overall, with z the charge state

$$Q_{\mathrm{i}} = \left(E_{\mathrm{inc}} - \frac{3}{2}k_{\mathrm{B}}T_{\mathrm{m}}\right) + \left(\sum_{i=1}^{z} U_{\mathrm{iz}}(i) - zW_{\mathrm{f}}\right) + U_{\mathrm{sb}}$$

- *In presence of electron emission, ion backscattering, sputtering,* the average exit energies of the emitted particles need to be subtracted together with the binding energy contribution (work function, surface binding energy and vaporization enthalpy, respectively). Introducing a cooling term

$$-Q_{\mathrm{c}} = \gamma\left(\bar{E}_{\mathrm{IIEE}} - \frac{3}{2}k_{\mathrm{B}}T_{\mathrm{m}} + W_{\mathrm{f}}\right) + R\left(\bar{E}_{\mathrm{ibs}} - \frac{3}{2}k_{\mathrm{B}}T_{\mathrm{m}} + U_{\mathrm{sb}}\right) + Y\left(\bar{E}_{\mathrm{sp}} - \frac{3}{2}k_{\mathrm{B}}T_{\mathrm{m}} + h_{\mathrm{v}}\right)$$

with γ the ion-induced electron emission yield, R the ion backscattering yield and Y the sputtering yield.

$$\bar{E}_{\mathrm{PEE}} = (U_{\mathrm{iz}} - 2W_{\mathrm{f}})/2 \qquad \bar{E}_{\mathrm{KEE}} = 2\,W_{\mathrm{f}} \quad \bar{E}_{\mathrm{ibs}} \sim 0.5E_{\mathrm{inc}} \quad \bar{E}_{\mathrm{sp}} \sim U_{\mathrm{sb}}$$

Surface processes

Non-plasma induced electron emission (thermionic emission only)

Thermionic emission

- Thermionic electrons are bound electrons that are ejected to the ambient from the interior of a metallic body mainly as a consequence of their thermal agitation.
- In thermionic emission (TE), electrons are mainly emitted by an entirely classical over-the-barrier mechanism when their normal kinetic energy exceeds the height of the surface potential barrier. The free electron theory of metals (assuming a non-interacting Fermi gas) is typically employed for the derivation of key results.

- In general, there are different thermionic emission regimes that are dictated by the competition between quantum tunneling and over-the-barrier escape. The regimes can be formally defined in a plot of the surface temperature versus the accelerating field strength. If distinguishing between regimes is based on the field strength (*i.e.* at constant surface temperature)
  - Classical thermionic regime (no external accelerating *(for emitted electrons)* electrostatic fields)
  - Schottky regime (very weak external accelerating electrostatic fields)
  - Extended Schottky regime (weak external accelerating electrostatic fields)
  - Field-assisted thermionic regime (moderate external accelerating electrostatic fields)

  Last three of importance for future machines Tolias, M. Komm, S. Ratynskaia and A. Podolnik, *NME* **25**, 100818 (2020)

- The process is not quantified by a yield, since it is not caused by the incidence of particle fluxes. It is quantified by expressions for the emitted electron current density which strongly depend on the surface temperature, the material composition and the external normal electrostatic field.

Richardson-Dushman formula

$$J_{\mathrm{th}}(T_{\mathrm{s}}) = A_{\mathrm{eff}}\, T_{\mathrm{s}}^2 \exp\left(-\frac{W_{\mathrm{f}}}{k_{\mathrm{B}} T_{\mathrm{s}}}\right).$$

- The thermionic current density is very sensitive to the

i. material work function, since it quantifies the height of the surface barrier that is crossed by the valence electrons
ii. surface temperature of the body, since it quantifies the strength of the thermal excitations that lead to the over-the-barrier emission.

- Good thermionic emitters should have a low work function and a high boiling / melting point.

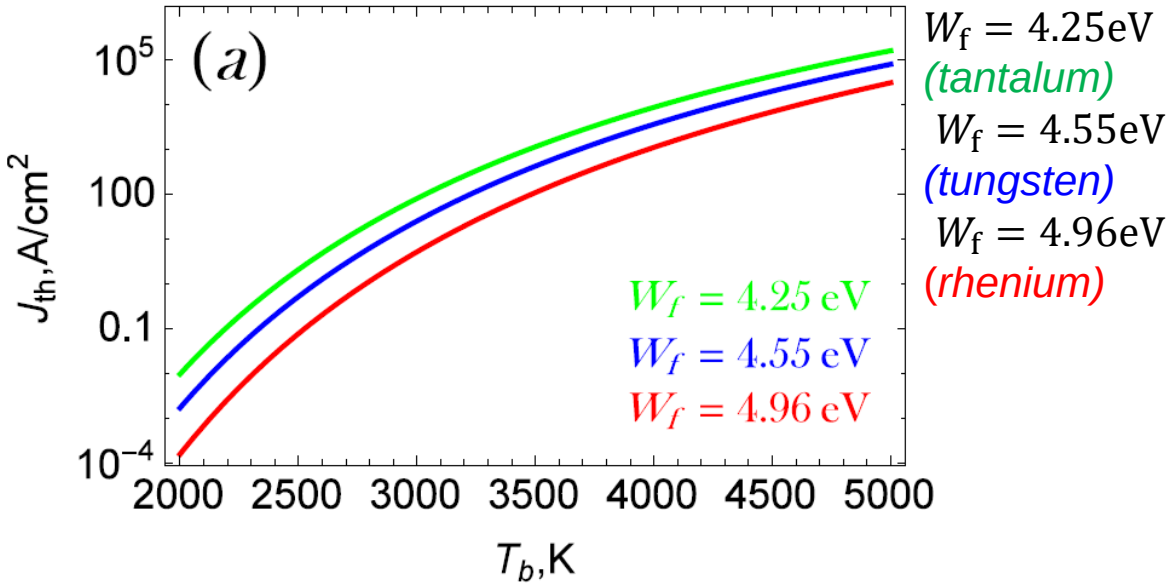

$W_{\mathrm{f}} = 4.25\mathrm{eV}$ *(tantalum)*
$W_{\mathrm{f}} = 4.55\mathrm{eV}$ *(tungsten)*
$W_{\mathrm{f}} = 4.96\mathrm{eV}$ *(rhenium)*

Surface cooling due to escaping thermionic electrons Γ_{th}

$$q_{te} = \Gamma_{th}(W_f + 2\, k_B T_s)$$

(filling the thermal vacancy)

NB: in plasmas escaping does not always follow Richardson-Dushman formula due to current limitation

Vapour pressure

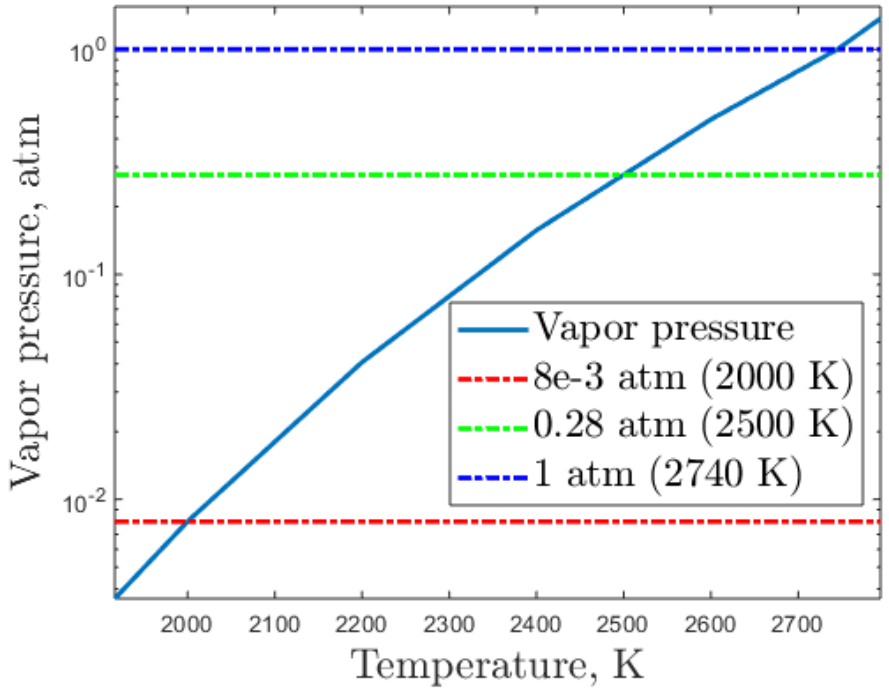

Particle-induced electron emission from tungsten